September 2004

INITIAL VHTR ACCIDENT SCENARIO CLASSIFICATION: MODELS AND DATA

R.B. Vilim
E.E. Feldman
W.D. Pointer
T.Y.C. Wei

Status Report

Nuclear Engineering Division
Argonne National Laboratory
9700 S. Cass Avenue
Argonne IL 60439

TABLE OF CONTENTS

LIST OF FIGURES

LIST OF TABLES

INITIAL VHTR ACCIDENT SCENARIO CLASSIFICATION: MODELS AND DATA

ABSTRACT

Nuclear systems codes are being readied under the Gen IV program as computational tools for conducting performance/safety analyses of the Very High Temperature Reactor. The thermal-hydraulic codes are RELAP5/ATHENA for one-dimensional systems modeling and FLUENT and/or Star-CD for three-dimensional modeling. We describe a formal qualification framework, the initial filtering of the experiment databases, and a preliminary screening of these codes for use in the performance/safety analyses.

Tables of important phenomena in the primary system indexed by operating regime and component are presented and prepare the ground for future preparation of Phenomena Identification and Ranking Tables (PIRT). The mixed convection mode of heat transfer and pressure drop is identified as an important phenomenon for Reactor Cavity Cooling System (RCCS) operation. We focused on the RCCS as a system for demonstration of our methodology. Scaling studies showed that the mixed convection mode is likely to occur in the RCCS air duct during normal operation and during conduction cooldown events. The RELAP5/ATHENA code was found to not adequately treat the mixed convection regime. Readying the code will require adding models for the turbulent mixed convection regime while possibly performing new experiments for the laminar mixed convection regime. Candidate correlations for the turbulent mixed convection regime for circular channel geometry were identified in the literature. We describe the use of computational experiments to obtain correction factors for applying these circular channel results to the specialized channel geometry of the RCCS. The intent is to reduce the number of laboratory experiments required. The FLUENT and Star-CD codes contain models that in principle can handle mixed convection but no data were found to indicate that their empirical models for turbulence have been benchmarked for mixed convection conditions. Separate effects experiments were proposed for gathering the needed data.

In years two and three we will move beyond mixed convection in the RCCS to similarly analyze other components and phenomena that are identified as important by the PIRTs. This is consistent with the project objective of identifying weaknesses or gaps in the code models for representing thermal-hydraulic phenomena expected to occur in the VHTR both during normal operation and upsets, identifying the models that need to be developed, and identifying the experiments that must be performed to support model development.

I. INTRODUCTION

The Very-High-Temperature Reactor (VHTR) is one of six reactor technologies chosen for further development by the Generation IV International Forum. In addition this system is the leading candidate for the Next Generation Nuclear Power (NGNP) Project in the U.S which has the goal of demonstrating the production of emissions free electricity and hydrogen by 2015. In preparation for the thermal-hydraulics and safety analyses that will be required to confirm the performance of the NGNP, work has begun on readying the computational tools that will be needed to predict the thermal-hydraulics conditions and safety margins of the reactor design.

The objective of the present multi-year project is to perform the following tasks in connection with the above nuclear systems codes and their use in safety analysis: (a) develop a formal qualification framework, (b) initial filtering of the existing databases and (c) preliminary screening of tools for use in thermal-hydraulics and safety analyses. It is expected that as an outcome of these tasks we will have 1) identified the systems codes to be used, 2) identified weaknesses or gaps in the code models for representing thermal-hydraulic phenomena expected to occur in the VHTR both during normal operation and upsets, 3) identified the models that need to be developed and the experiments that must be performed to support model development, and 4) will have identified the scaled experiments needed for validation of models. The project has been initiated within the framework of the Generation IV Nuclear Energy Systems Initiative in the area of System Design and Evaluation under the Work Package, A0802J01 "Modeling Improvement".

The computer codes to be used in the gas reactor performance and safety analysis can be divided into two groups, one-dimensional (1-D) system type codes and multi-dimensional computational fluid dynamics (CFD) codes. The choice of one over the other in an application involves first identifying the main phenomena and from this the dimensionless numbers that characterize the phenomena and their values. The suitability of a code is then judged in part by whether models for the phenomenon exist and whether they include the dimensionless numbers in a correlation valid for the values identified. While CFD codes can in principle be equipped to model all phenomena for which the 1-D codes are suited, the substitution of the former for the latter in every application is not practical. CFD codes require more detailed problem definition input and require orders of magnitude more computational time.

Both types of codes can be reviewed using the same approach since both are conservation law based and both contain empirical models (i.e. correlations of dimensionless numbers) that are the subject of the validation. The codes differ primarily in the level of detail present in the models to describe the underlying processes and, hence, in the types of experiment datasets needed to calibrate the models. For 1-D codes, validation is achieved using integral experiments that agglomerate over more than one fundamental phenomenon. For CFD codes a separate effects experiment focuses on a single phenomenon. Once validation for fundamental phenomena is demonstrated, validation can be complemented by comparison with integral phenomena experiments. In this report

we therefore use the same methodology to evaluate the models in each type of code but distinguish between the two types of experiment datasets.

This report describes work completed in the first year of this project. An approach was developed for reviewing code model adequacy. It provides a thorough and systematic treatment of all possible plant operating scenarios and related phenomena and ensures that all important design issues have been identified, and that the modeling needs are evident. To demonstrate the concepts and show how the work will proceed in years two and three, we step through for a single phenomenon the sequence for assessing the adequacy of the models. The case examined involves pressure drop and heat transfer in the mixed convection mode in a 1-D systems code. We use dimensional scaling to determine the presence of this phenomenon as a function of component and upset event. Where mixed convection is shown to occur, we examine the adequacy of the 1-D system code for modeling it. If a model is lacking we identify the experiments needed to support the required model development.

II. VERY HIGH TEMPERATURE REACTOR

The Very High Temperature Reactor (VHTR) is an extension of the earlier Gas Turbine-Modular Helium Reactor (GT-MHR). The GT-MHR [1] is a 600 MWt direct cycle gas reactor with a reactor outlet temperature of 850 ^{o}C. An isometric view is shown in Fig. 1. The VHTR differs mainly in that the target reactor outlet temperature is higher at 1000 ^{o}C and the VHTR is to produce hydrogen in addition to electricity. The main components of the VHTR are shown in Fig. 2 and include heat transfer equipment for the production of hydrogen. The arrangement of the heat exchanger for hydrogen production shown in Fig. 2 is only one of several possibilities under study. Additional details on the prismatic core and the Reactor Cavity Cooling System (RCCS) are provided below. The RCCS is included here as it has been selected as the system for demonstration of the filtering methodology described in this report. This was outlined in the introduction. While the Pebble Bed VHTR option is not discussed here, its design also includes an RCCS.

The VHTR is also referred to as the Next Generation Nuclear Plant (NGNP) [2] in this report.

A.   Prismatic Core

The reactor core consists of an inner reflector region surrounded by an annulus of fuel elements which is in turn surrounded by an annulus of outer reflector elements. The fuel elements are composed of hexagonal columns of graphite with circular holes that run the length of the column. The fueled holes contain fuel micro spheres while the coolant holes align axially to form coolant channels. A fuel element is shown in Fig. 3. Some important dimensions and conditions related to the coolant channels are given in Table I.

B.   Reactor Cavity Cooling System

The RCCS serves to remove heat from the exterior of the reactor pressure vessel during both normal and off-normal conditions. During normal operation the interior surface of the reactor pressure vessel is cooled by the reactor inlet coolant. If heat were not removed from the exterior of the vessel, the temperature distribution across the thickness of the vessel wall would be uniform and the same value as that of the reactor inlet coolant. Cooling the exterior of the vessel reduces the vessel temperature to a sufficiently low value to ensure its operational longevity. The RCCS extracts the heat from the exterior surface of the reactor vessel and transports it outside of the containment building. During off-normal accidents of extremely low probability all of the decay heat generated in the reactor is transferred to the reactor vessel wall and ultimately removed by the RCCS.

In the RCCS design, heat is radiated from the exterior of the reactor vessel wall to a series of heat exchangers that are oriented vertically and arranged in a circle around the exterior of the reactor vessel. Air flowing within these heat exchangers transports the heat to the exterior of the containment. The air is ducted in from outside the containment to these heat exchangers and then outside the containment. The heat exchangers are rectangular ducts with a large aspect ratio and arranged so that one of the short sides faces the reactor vessel. This requires that the flow exiting the heat exchangers be ducted to chimneys leading to the outside to induce a sufficient natural draft. The walls of the heat exchangers and the ducts that connect to them provide a barrier that separates the coolant flowing through the heat exchangers from the atmosphere inside the reactor containment. The air version of the RCCS system is designed to be totally passive under all operating condition and has no blowers to power the air flow through the heat exchangers. Fig. 4 is a schematic of the RCCS. There are 292 risers, each a 5 by 25.4 cm rectangular duct. There is a 5 cm gap between adjacent risers and the short sides of the riser face the reactor vessel and downcomer. The full power thermal-hydraulic conditions are given in Table II.

III. METHODOLOGY

The method we apply for NGNP thermal-hydraulic code qualification is related to the best estimate plus uncertainty method developed in the late 1980's for safety analysis of light water reactors (LWR). The Code Scaling, Applicability, and Uncertainty (CSAU) procedure [3] was used to conduct performance analyses of the Emergency Core Cooling System (ECCS) on a best-estimate basis rather than applying bounding conservatisms as had been the case previously. The method provided a systematic means for quantifying the uncertainty in the code predictions for severe loss of cooling accidents.[4] The process involves identifying the physical phenomena, selecting the key safety criterion, characterizing the phenomena in terms of scaled or dimensionless quantities, use of experiments with similar scale to assess accuracy of models in code, and finally making an estimate for the uncertainty in model prediction. The method was subsequently adapted for use in code development and improvement where the objective is ensuring

3

the code can model the plant behavior. Since that is very nearly our objective we have borrowed from that work.

There are differences between the issues addressed for LWRs and those important for the NGNP. For the LWR the requirement was sufficient confidence in the uncertainty in the code predictions that a reliable estimate could be made for accident damage and resulting release rate. The objective of the safety analysis was protection of the public. For the NGNP, however, the passive safety characteristics of the reactor are deemed to result in no significant fuel failure and, hence, negligible risk to the public. The objective is to confirm that for even the most serious events there is no significant release. With this shown, the question of risk to plant investment produced by elevated temperatures that shorten component lifetimes becomes an issue to confirm. Reactor and safety system performance is therefore also included as an objective in this exercise.

In a gas thermal reactor the dominant thermal-hydraulic phenomenon remain essentially unchanged ranging from normal operation to the severest accidents. No coolant phase change occurs and the fuel does not melt. As a consequence there likely will be no equivalent in the NGNP to the LWR experimental programs that involved hundreds of man years of analysis effort aimed at characterization and modeling of post-accident heat removal. Instead, the conditions that accompany the most severe gas reactor accident are a perturbation on normal operation. As a consequence the code qualification process should be simpler.

The goal is to identify the model improvements needed for the computer codes so that the codes properly represent the phenomena and can be used to address safety and design issues. This task has been broken into four steps: phenomena identification and ranking, modeling and scaling analysis, code review, and experiments. In the *phenomena identification and ranking* step we transition from an upset based means of identifying phenomena to an operating regime and equipment based approach. There are countless numbers of upsets of varying severity while there are only a limited number operating regimes and plant equipment components. Operating in terms of the latter provides increased assurance that all cases have been covered. In the *modeling and scaling analysis* step, it is assumed we have a specific phenomenon occurring in a specific component. The task is to determine an appropriate model to describe the phenomenon. We do so by first performing a scaling analysis to identify the dimensionless numbers that characterize the phenomenon. We then identify models that have been correlated in terms of these quantities and that provide a quantitative representation of the phenomenon. Should no model be identified, then we note this for consideration shortly. Assuming an acceptable model has been identified we move to the *code review* step where we examine the computer code with respect to modeling the phenomenon. If the model proves deficient we identify the model from the *modeling and scaling analysis* step, if was found, as being better suited. If no model was identified we move to the *experiment* step where we attempt to identify an existing experiment that could serve as a basis for deriving a model. If no experiment can be identified, then we indicate this as a development need. Fig. 5 is schematic of this process.

In the first year of this project we have illustrated the overall methodology from start to finish by working through a limited number of phenomena.

IV. PHENOMENA IDENTIFICATION AND RANKING

A key task is the identification of phenomena and plant components that are important to the plant response to accidents initiators. A ranking of phenomena and components as to their influence on process variables that have a safety or design limit can be used to identify the code models that figure most prominently. Since code prediction accuracy is most sensitive to these models, this is where effort to quantify code uncertainty and to reduce it should be concentrated. Focusing on these models ensures efficient allocation of resources.

A. Performance/Safety Criteria and Issues

A performance/safety analysis answers the question of whether performance/safety criteria specified for an accident class are met by the design. There are several accident classes. To simplify work in year one, detailed analysis associated with demonstration of our methodology was limited to the Loss of Forced Cooling (LOFC) or "conduction cooldown" class of events. In the present section then conduction-cooldown is a vehicle for illustrating how accident safety criteria drive the development of Phenomena Identification and Ranking Tables (PIRT). The PIRT will identify mixed convection in the RCCS as an important phenomenon-component pair.

The safety criteria for conduction cooldown are as follows. In this event the heat transport system and the shutdown cooling circulator system are inoperable. The safety objective is for the RCCS to serve as the ultimate heat sink in LOFC events. The main safety criteria are that it has the capability to limit the maximum fuel temperature to less than 1600° C and the maximum vessel temperature to less than 425° C pressurized and 530° C depressurized. The criteria are based on material properties. The PIRT should identify those phenomena and components that are important to remaining within these limits.

Safety issues arise in connection with questions about whether safety criteria can be met. Fig. 6 shows the factors that play into whether or not there is a safety issue. There are several factors: the design basis event which implies the transient phases and operating regimes, the phenomena occurring in the different plant components, and the material limits which are based on permissible temperature and rate of change of temperature in these components. Properly addressing safety issues requires these factors be considered. It is no surprise then that they appear in the course of generating a PIRT.

B. Operating Regimes

The plant behavior for each of the duty cycle, design basis, and beyond design basis events for which the safety analysis is performed consists of a number of operating

regimes or phases. Operating regimes prove useful in developing PIRTs because they more directly correlate with an important phenomenon and a safety criterion than do the individual duty cycle, design basis, and beyond design basis events.

Operating regimes are deduced by starting with a procedure outlined in [5]. All duty cycle, design basis, and beyond design basis events are subsumed by one of five classes with the result that no event should be inadvertently left out. The classes are reactivity insertion, loss of heat sink, loss of flow, overcooling, and flow runup. Not all events need to be explicitly listed since these classes have a single event that bounds the severity of conditions for all events in the class. Having listed these classes one then examines what key features describe the thermal-hydraulic regime the reactor is operating in. This is a function of three variables: pressure, cooling mode, and heating mode. As shown in Fig. 7, for these variables, respectively: the reactor is pressurized or depressurized; there is net flow through the core or there is only internal re-circulation; and the core is neutronically critical or is shutdown and producing decay heat. Table III gives the values of these features for all classes of duty cycle, design basis, and beyond design basis events. Table IV rearranges this information giving the event classes in each operating regime.

C. Phenomena and Components

The phenomena in the gas reactor, both expected and hypothesized, are listed in Table V. This list was compiled after reviewing a number of references dealing with gas reactor behavior [Appendix A] and after discussions with several knowledgeable sources [6,7]. Also shown are safety issues that are expected to arise with each of the phenomena. The phenomena and safety issues in Table V are general and given without reference to a specific gas reactor design or operating regime.

En route to developing a PIRT we must consider not only phenomena but also the component where the phenomena occur. The components in the NGNP primary system appear in Fig. 2.

D. Pre-PIRT Process

We completed preliminary steps to organize our work in preparation for development of the PIRTs in year two. For each operating regime identified in Table IV we reviewed the list of phenomena in Table V and used our judgment as to which phenomena are important in each component. The result appears in Table VI. In Table VII we expand on this to show the safety issues that are expected arise. Table VII is only a partial listing of the entries in Table VI. It will be completed in year two. The next step is to use this pre-PIRT process to structure and fill out the PIRT.

The structure of the PIRT is shown in Table VIII. The "component" and "phenomena" labels are coincident with our use of these terms. One also sees that the transient is broken into a sequence of operating regimes. To date we have focused on individual operating regimes without regard for how they might be connected. That compilation is to take place in year two.

V. MODELS AND SCALING ANALYSIS

A wide body of literature deals with the problem of extending the applicability of experimental data taken under a limited set of conditions to a more general set of conditions.[8,9] Methods such as dimensional analysis and scaling analysis have important applicability in gas cooled reactor design work. They can be used as a basis for conducting tests on a small scale with a less expensive representation of a thermal-hydraulics system and then extrapolating the results to predict the behavior of the full size system. They can also be used as a basis for developing relationships among thermal-hydraulics variables that are independent of physical dimensions and material properties thus leading to wide spread applicability. Such relationships are referred to as empirical or correlated models and appear in the RELAP5/ATHENA, FLUENT, and Star-CD codes. A main task of this project is to identify such models and to review their applicability to the phenomenon the codes will be called on to represent.

There are a generic set of issues that arise whenever correlated models are to be used in a safety analysis. We describe them as they are the sort of issues that drive the code applicability studies and will need to be addressed to some degree. A first issue is, are there distortions of processes introduced by conducting tests in scaled-down mockups? A designer attempts to maintain geometric, kinematic, and dynamic similarity between physical processes occurring at full-scale and those taking place in the scaled-down model. In general, exact similitude cannot be achieved and compromises are required. For these the designer uses engineering judgment to optimize similitude for the processes of greatest importance. This may introduce scale distortions of other less important processes or may introduce spurious processes which are atypical of the full-scale facility. A second issue is, in the course of fitting an empirical correlation and parameters to obtain agreement with experimental data, are there compensating errors introduced that under certain scenarios the corresponding compensating effects produce non-conservative results? A third issue is, are there correlations that are not supported by experimental data or are based on data which do not cover the range of interest in the analysis?

In this section the task is, for each instance of phenomenon and associated operating regime and component listed in Table VII, to identify the dimensionless numbers that characterize the related behavior. The general approach is to consider the field equations of conservation and transport. In particular the mass, energy, and momentum conservation equations are non-dimensionalized using an appropriately chosen set of scaling parameters. This yields dimensionless parameters as the sole parameters upon which the solution depends. Hence, if experimental data can be obtained from which one can infer the functional relationship among these dimensionless parameters, then one has an empirically correlated model for the phenomenon without regard to specific dimensions, thermal-hydraulic conditions, or material properties. In this section we describe the derivation of these models for heat transfer and fluid flow in mixed convection regime in the RCCS. In follow-on work in this project, this exercise must be repeated for the other entries in Table VII.

7

A.   Integral Phenomena

We refer to those processes that consist of more than one basic heat transfer or fluid phenomenon as *integral phenomena*. We are interested in their combined behavior and so seek a model that reflects this rather than an individual model for each of the phenomenon. As a result, the model does not contain explicit reference to each of the underlying processes, only a cause and effect type reference to the overall behavior. When the underlying processes are multidimensional the model captures only the net effect and provides no details on the nature of the multidimensionality. It is up to the correlation developer to note the conditions under which this aggregated representation is valid and then up to the user to observe them.

In this subsection, we identify requirements for correlated models for description of heat transfer and pressure drop in the mixed convection regime in the RCCS under regime OR6 - *Depressurized/ Conduction Cooling/ Shutdown Decay Heat* given in Table VII. The suitability of models in RELAP5/ATHENA for predicting this phenomenon under these conditions is determined in the next section.

The heat transfer and pressure drop within the riser are treated as integral phenomenon. During depressurized conduction cooling conditions the axial component of the riser velocity field will have a two dimensional spatial dependence in the horizontal plane. As a result the local heat transfer coefficient and wall friction will vary around the circumference of the duct. Additionally, at the low flowrates both forced convection and natural convection heat transfer, so-called mixed convection heat transfer, may be present. Despite these multi-phenomenon, multi-dimensional elements, one can treat the mass, energy, and momentum balances for the air in the riser as one-dimensional. In so doing, one must derive integral correlations for heat transfer and friction that do not explicitly model local phenomenon that control these such as the boundary layer thickness and turbulence.

The dimensionless parameters that appear in correlated models for describing one-dimensional pressure drop and heat transfer rate are derived from the non-dimensionalized conservation equations. Below we present a summary of results for heat transfer and pressure drop for in laminar flow forced convection between two vertical parallel plates. The implication is that mixed convection, the combination of both forced and natural convection, will depend on the same dimensionless parameters. The analysis below is representative of the types of analyses that should underlie the identification of dimensionless parameters for the phenomenon in Table VII.

A.1   Dimensionless Parameters

We consider two stationary vertical parallel plates with fluid between them. Assume x is the distance along the direction of flow and y is the distance along the normal to the plates. Assume the plates are separated by the distance $2 y_0$.

For *pressure drop for fully developed laminar flow,* the conservation of momentum equation is [9]

$$\frac{dP}{dx} = \mu \frac{d^2 v_x}{dy^2} \tag{1}$$

where P   =   pressure,
μ   =   coolant viscosity, and
v_x =   fluid velocity in direction of flow

where the coolant density, ρ, and viscosity are constant. The velocity v_x is solved for

$$v_x = \frac{3}{2} V \left[1 - \left(\frac{y}{y_0} \right)^2 \right] \tag{2}$$

and integrated to give the average velocity

$$V = -\frac{1}{3\mu} \frac{dP}{dx} y_0^2 \ . \tag{3}$$

Now define a dimensionless variable, the friction factor

$$f = \frac{-\Delta P}{\frac{\Delta x}{y_0} \frac{1}{2} \rho V^2} \ . \tag{4}$$

Eqs. (3) and (4) combine to give

$$f = \frac{6}{Re} \tag{5}$$

where $Re = \rho V y_0 / \mu$ is the Reynolds number.

For *heat transfer for fully developed laminar flow*, the temperature satisfies [9]

$$\rho C_p v_x \frac{\partial T}{\partial x} = k \frac{\partial^2 T}{\partial y^2} \tag{6}$$

where k is thermal conductivity, C_p is specific heat, and T is temperature and can be solved for analytically. Let the temperature of the two plates be T_0 and T_1, respectively. One defines a heat transfer coefficient

$$h = \frac{q''}{T_0 - T_m} = \frac{k \left(\frac{\partial T}{\partial y}\right)_{y=y_0}}{T_0 - T_m} \tag{7}$$

where T_m is the mixed mean fluid temperature obtained by averaging the velocity weighted temperature profile normal to the direction of flow. The above expression is rearranged and a new quantity, the Nusselt number defined,

$$Nu = \frac{h \, y_0}{k} = \frac{\partial \left(\frac{T - T_m}{T_0 - T_m}\right)}{\partial \left(\frac{y}{y_0}\right)} \quad . \tag{8}$$

Since the temperature T exists as an analytic expression obtained by solving Eq. (6), then the right-side of Eq. (8) can be evaluated. Hence, the heat transfer coefficient is a function of the Nusselt number, a dimensionless quantity.

For *heat transfer for natural convection laminar flow*, assume that the plates have infinite extent in the x direction, that the temperature is independent of x, and that axial conduction and friction effects can be neglected. Then in the fully developed region the temperature is given by [9]

$$\frac{d^2 T}{dy^2} = 0 \, . \tag{9}$$

If the temperature of the plates are T_0 and T_1, respectively, then

$$\frac{T - T_m}{T_1 - T_m} = -\frac{y}{y_0} \, . \tag{10}$$

The velocity is given by the momentum equation with a term to account for buoyant forces [9]

$$\frac{\mu \, \partial^2 v_x}{\partial y^2} + \rho \beta g_x (T - T_m) = 0 \, . \tag{11}$$

The above equation solved for the velocity with the temperature given by Eq. (10) and $v_x = 0$ at the face of the plates gives

$$v^* = \frac{1}{6} Gr \, Pr \, (y^{*3} - y^*) \tag{12}$$

where

$$v^* = \frac{v_x \rho C_p y_0}{k} \,, \qquad\qquad \text{dimensionless velocity}$$

$$Gr = \frac{g \beta y_0^{3} (T_1 - T_m)}{\nu} \,, \qquad\qquad \text{Grashof number}$$

$$y^* = \frac{y}{y_0} \,. \qquad\qquad \text{dimensionless length}$$

The linear temperature profile was obtained for negligible friction. This will be the case for low GrPr as described in [9]. Thus, Eq. (12) is valid only for low GrPr.

The heat transfer coefficient is from Eq. (7) and (10) given by

$$Nu = \frac{h\, y_0}{k} = 1 \,. \tag{13}$$

As GrPr increases and frictional losses become important, the temperature profile given by Eq. (9) will no longer be valid. The temperature and velocity profiles will become interdependent. The velocity profile will maintain a Gr number dependence and so the heat transfer coefficient given by Eq. (8) will assume a Gr number dependence.

A.2   Regime Map

In the mixed convection region both natural convection and forced convection are present. We expect then that the correlation of pressure drop and heat transfer under mixed convection laminar flow conditions will exhibit those same dimensionless numbers derived for laminar flow above using simple conservation balances. See Table IX for a summary of the above results. Thus, models for describing pressure drop and heat transfer in this regime should include a dependence on the quantities Re, Pr, Gr, and y* presented in Table IX. As a corollary experiments for obtaining correlations for pressure drop and heat transfer in the mixed convection regime should include Re, Pr, Gr, and y*.

It has been found that the demarcation among natural, mixed, and forced convection is given by values of a subset of these dimensionless numbers. Fig. 8 is a regime map for circular tubes and shows the dependence of the regime on Re, Pr, Gr, and y*.

We investigated the likelihood that core channel flowrate or RCCS duct flowrate are in the mixed convection region during either normal or off normal operation. If so, then the 1-D system code used for accident analysis must have appropriate correlations for heat transfer and pressure drop. The correlations should include a Re, Pr, Gr, and y* dependence as described above. The calculation of Re and Gr for an average core channel both at full power and at shutdown with the shutdown circulator running under pressurized and depressurized conditions is given in Tables X and XI, respectively. The

dimensionless numbers for the axes of the Fig. 8 regime map are shown in Table XII. Plotting the values from this table on the regime map shows that the channel condition remains solidly in the forced convection region.

For the RCCS air duct, the calculation of Re and Gr at full power is given in Tables XIII and XIV, respectively. From these tables we have Re = $1.4*10^4$ and Gr*Pr*D/L ~10^7 where we have taken D/L = 0.01. This point falls just inside the mixed convection region in Fig. 8. During shutdown the point will move diagonally since the flowrate (Re) is positively correlated with the power (Gr). Whether the point moves down and to the left or in the opposite direction depends on the details of the transient and can be answered with a 1-D systems code simulation. In either case, the air in the duct will trace a path through the mixed convection region. Since the duct is non-circular and the heat flux is not uniform while Fig. 8 is for vertical heated pipes, the exact path might be better determined from a flow regime map specific to the geometry and heating conditions.

A.3   Models

The pressure drop in a vertical round pipe in the turbulent flow regime is altered when wall heating is introduced. The heating of the fluid at the wall introduces buoyant forces which change the velocity profile and affect the pressure drop. The pressure drop can increase or decrease depending on the conditions. The correlation of Petukhov [10] expresses the friction factor of the heated case in terms of the unheated case. For conditions where Pr > 0.6, Re > 3000, 0< Gr < 10^{11}, and L/D > 40 the heated friction factor is given by

$$f = \left[\frac{1 + 0.83\,e^2}{f_0^{-1/2} + 0.076e^2 E^{1/4}} \right]^2 \tag{14}$$

where

$$e = \frac{10^3\,Gr}{\mathrm{Pr}\cdot \mathrm{Re}^{2.75}} \quad , \quad E = \frac{Gr}{\mathrm{Pr}\cdot \mathrm{Re}^4} \tag{15}$$

and the unheated friction factor is given by

$$f_0 = \left[1.82 \log_{10} (\mathrm{Re}/8) \right]^{-2}. \tag{16}$$

The heated friction factor is plotted in Fig. 9 against Grashof number for different values of Reynolds number. One sees that the friction factor drops below the value of the unheated case for initially small heating rates but then rises above for increased heating. We have also plotted the condition in the RCCS air duct at the full power condition. Fig.

9 shows that the pressure drops to 0.8 of the value for the case where there is no heating, all other things being equal. After shutdown, the condition in the duct will move away from the full power point shown on Fig. 9. Proper prediction of the RCCS response by safety analysis code requires then that mixed convection pressure drop in the turbulent regime be treated as a case distinct from the forced convection case.

Similarly, the heat transfer coefficient at the wall of a pipe with vertical upflow is altered when buoyant forces in the fluid appreciably change the fluid velocity profile in the pipe. A discussion of this phenomenon is given in [11]. Briefly, the buoyant forces induced in the fluid nearest the wall by heating of the exterior of the wall increase the fluid velocity near the wall over the case of no heating. Mass conservation implies that the velocity near the centerline decreases for a net flattening of the velocity profile. This is referred to as aiding flow. The opposite, cooling of the wall, gives rise to opposing flow. Both are shown schematically in Fig. 10 [11]. If the flow is turbulent in the non-heated case, arguments based on Prandtl's mixing model suggest that heat transfer is reduced by heating. The effect on heat transfer coefficient is shown in Fig. 11 [11]. If the flow in the unheated case is laminar, then heating gives the opposite effect. [12]

To summarize, there are two independent dimensions to heat transfer for single-phase flow. First we have the heat transfer mode which can be forced, mixed, or natural convection. Second we have the flow regime which can be laminar, turbulent, and transition between laminar and turbulent flow. One can considered a two dimensional array for heat transfer in which one dimension represents laminar, transition, and turbulent flow and the other represents free, mixed, and forced convection. One obtains a nine-region, three-by-three array. The situation for friction factor is identical.

An assumption we have made is that the flow and temperature boundary layers are fully developed. This, of course, can only be an idealization. However, flow channels in reactor applications tend to be hundreds of diameter long whereas fully developed flow is attained within tens of diameters. A further consideration, of particular importance for laminar flow, is the shape of the channel. Although, the law-of-the-wall makes behavior of turbulent flow relatively insensitive to channel shape, this is not true for laminar flow, even for the simplest of case of forced laminar flow.

B.   Separate Effects

We refer to those processes that consist of only one basic heat transfer and/or fluid dynamics phenomenon as *separate effects*. The ability to accurately predict the behavior of a single separate effect is critical if we are interested in capturing the multidimensionality of underlying processes in the analysis of integral phenomena. Since the number of separate effects problems that could be identified for any system is almost unlimited and the end goal is to use the separate effects modeling capability to predict the multidimensional behavior of important integral phenomena, it is highly desirable to make use of a generic multidimensional modeling capability that is valid over some limited range of conditions rather than developing many approaches that are highly specialized for each separate effect of interest. Like the integral effects correlations, it is

up to the model developer to note the conditions under which each representation of heat transfer and/or fluid dynamics behavior and the user to observe them.

In this subsection we identify requirements for correlated models for use in the prediction of separate effects which may impact the performance of the RCCS under regime OR6 – *Depressurized/Conduction Cooling/ Shutdown Decay Heat* given in Table V. The suitability of models available for computational fluid dynamics (CFD) analysis of the RCCS components under these conditions is discussed in the next section.

As stated in the previous subsection, the axial component of the riser velocity field will have a two dimensional spatial dependence in the horizontal plane during depressurized conduction cooling conditions. As a result, the local heat transfer coefficient and wall friction will vary circumferentially around the duct. Furthermore, the flow of fluid through the riser is driven entirely by thermally-induced density gradients, and flow rates through the duct are relatively low. Consequently, a mixture of natural and forced convection heat transfer as defined based upon the flow rate through the duct rather than the nature of the driving force may occur. Where there is a need to understand the multidimensionality of the flow field within the duct, the local separate effects phenomena that generate turbulence and trigger changes in boundary layer thickness must be modeled explicitly.

The Navier-Stokes equations, the mathematical representations that are employed in the CFD modeling of heat transfer and fluid dynamic phenomena, are derived from the basic conservation equations and provide a complete generic solution to any fluid dynamics and heat transfer problem. However, the application of the Navier-Stokes equations in their full detail is impractical for most flow fields, and especially for turbulent flow fields, so parameterized versions of the equations are typically employed. Empirical correlations are used to determine appropriate localized values for these parameters throughout the multidimensional domain. While dimensionless forms of the Navier-Stokes equations are know, dimensional forms are more commonly used since there is no need to try to reduce all important phenomena into a single dimensionless parameter. The parameterized form of the Navier-Stokes equations and the basic forms of the correlations that would typically employed for turbulent incompressible flow between two vertical parallel plates are discussed below. The implication of the formulation employed is that the features that are important to integral phenomena correlations, such heat transfer regime, are not as important to the accuracy of the correlated turbulence and boundary layer models as features that impact the growth of the boundary layer or development of turbulence, such as abrupt changes in geometry that result in a separated boundary layer.

B.1 Parameters

For any fluid flow field, the behavior of the flow field can be described exactly by the Navier-Stokes equations: [13]

$$\bar{\nabla} \cdot \bar{V} = 0 \tag{17}$$

$$\rho \frac{D\vec{V}}{Dt} = \rho\vec{g} - \vec{\nabla}p + \mu\nabla^2\vec{V} \tag{18}$$

$$\rho c_p \frac{DT}{Dt} = k\nabla^2 T + \tau'_{ij}\frac{\partial u_i}{\partial x_j} \tag{19}$$

where $\vec{V}$ = velocity vector

ρ = density

t = time

$\vec{g}$ = gravitational acceleration vector

p = pressure

μ = dynamic viscosity

c_p = specific heat

T = temperature

k = conductivity

τ'_{ij} = viscous stress tensor

u_i = velocity component i

x_j = coordinate direction j

If Reynolds' time-averaging approach is utilized and each variable is assumed to be composed of the sum of an average-valued component and a fluctuating component, such that any variable Q is described by:

$$Q = \overline{Q} + Q' \tag{20}$$

where the bar notation indicates the time average component and the prime notation indicates the fluctuating component, then the Navier-Stokes equations can be reformulated as the Reynolds-Averaged Navier-Stokes equations:

$$\vec{\nabla} \cdot \overline{\vec{V}} = 0 \tag{21}$$

$$\rho \frac{D\overline{\vec{V}}}{Dt} = \rho\vec{g} - \vec{\nabla}\overline{p} + \vec{\nabla} \cdot \left[\mu\left(\frac{\partial u_i}{\partial x_j} + \frac{\partial u_j}{\partial x_i}\right) - \rho\overline{u'_i u'_j} \right] \tag{22}$$

$$\rho c_p \frac{D\overline{T}}{Dt} = -\frac{\partial}{\partial x_i}\left(-k\frac{\partial \overline{T}}{\partial x_i} + \rho c_p \overline{u'_i T'}\right) + \overline{\Phi} \tag{23}$$

where $\mu\left(\dfrac{\partial u_i}{\partial x_j} + \dfrac{\partial u_j}{\partial x_i}\right)$ = laminar flow stress tensor

$\rho\overline{u'_i u'_j}$ = turbulent flow stress tensor

$\overline{\Phi}$ = total dissipation $\approx \dfrac{\partial \overline{u}}{\partial y}\left(\mu\dfrac{\partial \overline{u}}{\partial y} - \rho\overline{u'v'}\right)$

μ = dynamic fluid viscosity

The turbulent stress tensor is still unknown, but the equations are now presented in a form that lends itself to the development of "turbulence conservation" equations that may be used to relate the turbulent stresses to the mean flow field and facilitate the solution of the above equation set without the need to know the turbulent stress tensor *a priori*. The most commonly used "turbulence conservation" equation is the turbulent kinetic energy equation, where the turbulent kinetic energy is defined as

$$K = \tfrac{1}{2}\overline{u_i' u_i'}. \tag{24}$$

The turbulent kinetic energy equation can be derived by forming the dot product of u_i and the *i*th momentum equation then subtracting the instantaneous mechanical energy from its time averaged value to form:

$$\frac{DK}{Dt} = -\frac{\partial}{\partial x_i}\left[\overline{u_i'\left(\tfrac{1}{2}u_j'u_j' + \frac{p'}{\rho}\right)}\right] - \overline{u_i'u_j'}\frac{\partial \overline{u}_j}{\partial x_i}$$
$$+ \frac{\partial}{\partial x_i}\left[\overline{\nu u_j'\left(\frac{\partial u_i'}{\partial x_j} + \frac{\partial u_j'}{\partial x_i}\right)}\right] - \nu\overline{\frac{\partial u_j'}{\partial x_i}\left(\frac{\partial u_i'}{\partial x_j} + \frac{\partial u_j'}{\partial x_i}\right)} \tag{25}$$

where ν = kinematic viscosity = μ/ρ

Obviously, the terms of this relation are too complex to compute them from first principles and an engineering modeling approach will need to be applied.

B.2. Models

The most commonly applied modeling strategy is the two-equation high-Reynolds number K-ε model:

$$\frac{DK}{Dt} \approx \frac{\partial}{\partial x_j}\left(\frac{\nu_t}{\sigma_K}\frac{\partial K}{\partial x_j}\right) + \nu_t\frac{\partial \overline{u}_i}{\partial x_j}\left(\frac{\partial \overline{u}_i}{\partial x_j} + \frac{\partial \overline{u}_j}{\partial x_i}\right) - \varepsilon \tag{26}$$

$$\frac{D\varepsilon}{Dt} \approx \frac{\partial}{\partial x_j}\left(\frac{\nu_t}{\sigma_\varepsilon}\frac{\partial \varepsilon}{\partial x_j}\right) + C_1\nu_t\frac{\partial \overline{u}_i}{\partial x_j}\left(\frac{\partial \overline{u}_i}{\partial x_j} + \frac{\partial \overline{u}_j}{\partial x_i}\right) - C_2\frac{\varepsilon^2}{K} \tag{27}$$

where σ_K and σ_ε are effective Prandtl Numbers, which relate the eddy diffusion of K and ε to the momentum eddy viscosity ν_t. The eddy viscosity itself is modeled as

$$\nu_t = \frac{C_\mu K^2}{\varepsilon}. \tag{28}$$

Thus the turbulent fluctuations can be linked to the average velocity field using two equations containing five unknown constants that must be experimentally determined:

C_μ, C_1, C_2, σ_K and σ_ε. The recommended values for these empirical constants for calculations in which the boundary layer remains attached to the wall are shown in Table XV.

Equations 26 and 27 are combined with the continuity, momentum and energy equations to form a complete system of equations to describe turbulent shear flow. This form of the model neglects molecular viscosity and sub-layer damping effects, so it can only be used in the outer and overlap regions of the boundary layer. The behavior in the inner sub-layer is typically modeled using a logarithmic wall function of the form:

$$K = \frac{v^{*2}}{C_\mu^{1/2}} \tag{29}$$

$$\varepsilon = \frac{v^{*3}}{\kappa y} \tag{30}$$

$$\frac{\bar{u}}{v^*} = \frac{1}{\kappa}\ln\left(\frac{v^* y}{v}\right) + B \tag{31}$$

where y = distance from the wall
  κ = Kármán's constant $\approx$ 0.41
  v^* = wall friction velocity
  B = intercept from empirical data $\approx$ 5.0

This particular wall function form assumes that variations in velocity are predominantly normal to the wall, the effects of pressure gradients are negligibly small, and that a balance exists between turbulence generation and dissipation. These conditions are reasonable for turbulent incompressible flow between two vertical flat plates. Alternate forms may be applied when the flow field of interest is does not satisfy these conditions.

VI. CODE REVIEW

The nuclear safety codes are reviewed with respect to modeling requirements established in the previous section. The 1-D systems code is RELAP5/ATHENA and the CFD code is FLUENT. The selection of these codes as the thermal-hydraulic safety analysis tools for the NGNP design was made outside of this project. In this section, we review these codes below for each of the phenomenon examined in the previous section. For RELAP5/ATHENA we examine the treatment of mixed convection heat transfer and pressure drop. For FLUENT and Star-CD we review the available options for the modeling of turbulence.

A.   RELAP5/ATHENA

We found in the previous section that the mixed convection flow regime may be present in the air duct of the RCCS during both normal and off-normal operation. We described

instances where forced convection models applied to this regime under-predict pressure drop and over-predict heat transfer. Under these circumstances core fuel temperatures would be under-predicted. Since the RCCS has an important safety function in limiting fuel temperatures during accidents it is important that the thermal-hydraulics models in RELAP5/ATHENA include treatment of the mixed convection regime.

We reviewed RELAP5/ATHENA for the treatment of pressure drop and heat transfer in the mixed convection regime. The following appears on page 4-86 of Volume IV of the RELAP5/ATHENA manual: "There are other situations besides cooling that are *not accounted for*. These include entrance effects, laminar-turbulent transition and *mixed forced*, and free *convection*" where we have italicized text for emphasis. Correlations for Nusselt number are given in Section 4.2.2 starting on page 4-77 of Volume IV. In particular the table on page 4-80 indicates laminar and turbulent flows and natural convection, but no mixed convection. Correlations for friction factor are given in Volume I Section 3.3.8.6 starting on page 3-180 and also Volume IV Section 6.2.1.2 starting on page 6-40. No correlations are given for mixed convection.

B.   FLUENT and Star-CD

Fluent and Star-CD both offer a wide variety of turbulence modeling options, ranging from the very simplistic to the highly complex, as part of their standard suite of tools. For extremely simplistic flow fields, both codes offer the ability to utilize a single equation Prandtl mixing length model for the prediction of the turbulence field. For basic compressible or incompressible flow fields with reasonably isotropic turbulence and minimal boundary-layer seperation, both codes offer two-equation high and low Reynolds number K-ε models. Low Reynolds number models require a highly refined computational mesh near any wall in order to properly resolve the turbulence field all the way to the wall and can be computationally expensive in either code. High Reynolds number models require a separate wall function to resolve the turbulence field in the near wall region without the need for the highly refined computational mesh, and both codes offer a comparable selection of log-law and algebraic functions to address different surface characteristics.   Both codes also offer a comparable selection of alternate K-ε type models that include additional terms to improve the accuracy of the calculation of the dissipation.

For slightly more complex flow fields in which significant regions of the boundary layer are separated from the wall, both codes offer a comparable selection of two-equation K-ω models. As with the K-ε models, the K-ω models may be used to model the turbulence field to the wall with a highly refined mesh or in conjunction with a wall function when a coarser mesh is used.   For flow fields in which the turbulence is primarily anisotropic, both codes offer a selection of higher order two-equation models that include additional non-linear terms in the dissipation equation to account for the anisotropy.

Both codes also include a comparable selection of advanced modeling options which provide additional details about the turbulence field at the expense of significantly larger computational investment. The additional information may make these modeling options

more robust for flow fields which contain complex flow structures resulting from large regions of boundary layer separation, periodic vortex shedding mechanisms, impinging jet flows, or other pressure gradients normal to the surface. The only steady state modeling option among these models is the Reynolds Stress Models (RSM), which model each of the stresses in the stress tensor directly using algebraic formulations. Both codes also offer limited capability to utilize Large Eddy Simulation (LES), in which various formulations are used to model sub-grid turbulence while large turbulence structures are simulated directly, and Discrete Eddy Simulation, in which LES is employed in the far field and a K-ε or K-ω model is used near the wall to improve the accuracy of predictions in the near wall region. In the event that a suitable model is not included for a particular application, both codes offer the capability for the user to add a new model through pre-defined user subroutines.

VII. EXPERIMENTS

A. Initial Filtering of Existing Databases

We compiled a list of experiment databases by performing a search of the open literature for phenomena cited mainly in the context of gas reactors. In the future, we will widen our search criteria to include consultation with experts. The consultation will not be limited to the nuclear field but will include the aeronautics and chemical engineering industries.

We describe here only those experiments that are centered on the RCCS. Then in subsections VII.B1 and 2 we weigh the usefulness of these experiments with respect to specific needs identified in Section V for modeling RCCS phenomenon and we comment on the need for additional experiments.

References [14] and [15] provide experimental data pertaining to the RCCS of the JAERI (Japan) HTTR reactor. Both contain benchmark problems with experimental data that was used for code validation by various reactor development organizations around the world—Japan, Russian Federation, South Africa, United States of America, and France in the case of [14]. Each report provides experimental data and the analytical results provided by various modelers. Both reports provide steady-state axial distributions of reactor vessel temperature and cooling panel temperature. (The cooling panels are the mostly vertical air-to-air or air-to-water heat exchangers that receive the heat transferred from the exterior of the reactor vessel and enable it to be transferred from the reactor cavity.)

Reference [14] provides experimental data obtained directly from the HTTR reactor at two power levels—full power (30 MWt) and 9 MWt. The cooling panels are water cooled. Reference [15] describes an experimental mockup of the HTTR in which an electric heater that has six axial segments is used in place of the reactor core. It appears that no attempt was made to preserve similitude between the mockup and the HTTR reactor plant and the mockup is approximately a fourth the size of the HTTR, but is not to

scale. It appears that an adequate description of the experiment is provided. The data in Table XVI was copied from Table 4-0 of the reference. These are all steady state tests for which experimentally measured temperatures are provided graphically for the pressure vessel and the cooling panel. Based on the figure on page 12 of the reference, the control rod stand pipes are capped pipes that extend from the top of the reactor vessel and are used as conduits for the control rod drive handles.

The experimental data provided by the references is not specific with respect to geometry and conditions to the particular VHTR reactor under consideration in this report. Also these data would not be used to establish new fundamental relationships of general utility. However, there is considerable value in having measured data from facilities that have analogous systems and employ some of the same phenomena as those of the NGNP. Such data can be used very effectively by modeler and code developers to identify governing phenomena and modes of facility behavior that would otherwise have been overlooked. Of references [14] and [15], the latter appears to be the better of the two to use for such purposes. The facility for this reference is fundamentally simpler and the experiment is better described than in [14]. In both cases, it is not obvious that all of the details that one would need to do a thorough comparison with measured data are published, since the need for missing crucial details are often uncovered during the analytical process.

B. Measured Data Needs

    B.1   Integral Phenomena

We noted earlier that friction factor and heat transfer in the mixed convection regime occupy a subset of the elements in a three-by-three array with convection mode and flow regime as independent variables. A good review of existing correlations that populate this matrix is given in [12]. This review identifies for heat transfer a correlation each for constant heat flux and constant wall temperature conditions for each of the nine elements in the matrix. Where buoyancy is a factor the correlation is for up-flow. For friction factor the review identifies for forced convection correlations for turbulent, laminar, and transition regime. For mixed convection up-flow it identifies correlations for turbulent flow. These turbulent mixed convection regime correlations are candidates for filling the void in RELAP5/ATHENA identified in subsection VI.A. For mixed convection up-flow in the laminar flow regime [12] cites a lack of data or correlations.

It is not clear whether the absence of friction factor data for mixed convection up-flow in the laminar flow regime is a void that needs to be filled for RELAP5/ATHENA qualification. These low Reynolds numbers in the core channels will be reached long into a cooldown event. By that time and at these low flowrates the predominant mode of heat removal in the core may be radial conduction. Similarly, for the RCCS air duct these low Reynolds numbers might eventually be reached, but by then the primary system temperatures may have long ago peaked. In such a case, an error in the friction factor may have little consequence with respect to being able to make a reliable prediction that temperatures remain below safety criteria limits. Thus, before a recommendation can be

made as to the need for performing experiments for the mixed convection laminar flow regime, whole plant simulations should be performed to determine primary system temperatures far out in time when either core channel or RCCS air duct flows might be expected to be laminar.

With length to diameter ratios in the hundreds and Reynolds numbers in the thousands for these channels one would expect predominantly one-dimensional flow without recirculation. That is, pure natural convection is not expected at anytime where not having the corresponding correlations in place might be of consequence. Again this should be checked by performing a whole plant simulation, computing dimensionless numbers, and then examining the regime map of Fig. 8.

The RCCS air duct is decidedly two-dimensional in heat flux and channel shape. The error arising from applying circular tube correlations for heat transfer and friction factor must be quantified. In the event it is unacceptable, then a semi-scale experiment using the air duct geometry would be required to obtain integral data for heat transfer and friction factor.

B.2 Separate Effects

Since the turbulence models that are employed in multi-dimensional CFD simulations are generic in form and serve only to describe the relationship between the fluctuating and average components of any variable, any simulation regardless of turbulence model selection can be expected to provide some insight into the expected behavior of the flow field. Since engineering analyses are typically most interested in the characteristics of solid components under different system conditions, the accuracy of the simulation is typically judged by the ability of a model to predicted wall quantities of interest. Hence, the accuracy of the prediction of a specific separate effect is largely dependent on appropriateness of the selected turbulence model's treatment of the generation and dissipation of turbulence in the near wall region. Consequently, significantly more detailed data sets are needed for the assessment of turbulence model accuracy than for the assessment of one-dimensional correlations associated with integral phenomena.

While significant integral data exists for the mixed convection regime expected to dominate the performance of the RCCS, a comparable data set has not yet been identified for validation of multi-dimensional CFD simulations of compressible, mixed-convective flow in a vertical duct with heated boundaries that cannot be described as constant heat flux or constant temperature. In order to provide sufficient confidence of the ability of a turbulence model to adequately capture the turbulence field under such conditions, a suitable experiment must use a compressible coolant and be both heated and buoyancy-driven. The data collected from such an experiment must include measurements of the velocity, temperature, and turbulence parameter profiles across the duct cross-section for direct comparison with predicted values. Furthermore, the complexity of the thermal boundary condition requires that the surface temperature distribution be sufficiently well described for use as a boundary condition in the benchmarking calculations. An example

of the level of data detail needed for a separate effects validation of turbulence modeling capability can be found in the paper of Krauss and Meyer.[16]

C. Computational Data Needs

Engineering-scale experiments are the preferred means for acquiring data for qualifying models in a computer code. However, designing an experiment, assembling the equipment, and performing the experiment are costly and time consuming tasks. Therefore, prudence is required to limit the number of experiments to only the most essential As we describe below, one may be able to reduce the required number of experiments by relaxing the strict separation made in subsection VII.B between a 1-D code with integral experiments and a CFD code with separate effect experiments. We describe a cross over of models and data.

In the case of integral phenomena, the aggregation of spatial detail results in a model and measured data that are geometry specific. Geometric similitude allows generalization of measured data to different dimensions as long as aspect ratios are preserved. But for significant geometry changes, generalizing of results (e.g. extrapolation of results for 1-D uniform heat flux in a circular pipe to 2-D heat flux dependence in a rectangular duct) may introduce uncertainty that is not easily bounded without performing an actual experiment in the new geometry. Thus, there is an apparent need to perform geometry specific experiments in the case of the 1-D code models identified in subsection VII.B.1. This can lead to a large number of experiments.

In practice we may be able to limit the number of such experiments by replacing them with *in silico* or *computational* experiments. We use the case of a heated vertical flow channel with specialized cross sectional geometry, such as found in the air duct of the RCCS, as an example. This is a geometry perturbation on the *heated vertical circular pipe* experiment. Correction factors can be generated for obtaining the behavior of the heated flow channel with specialized cross sectional geometry from experiments and correlations for the simpler geometry described in the literature. If these correction factors for heat transfer coefficient and friction factor can be obtained from CFD calculations (i.e. numerical experiments) for the specialized geometry, then the number of required laboratory experiments is significantly reduced. This of course assumes that the CFD code has been first qualified for the relevant separate effects in this specialized geometry. These separate effects were described in subsection VII.B.2. A necessary test of the adequacy of the resulting capability is that the CFD code be able to replicate the measured integral behavior in the simpler geometry. Essentially, by this process, we are substituting computational data for measured data.

In summary, we expect the need for 1-D models of heat transfer and pressure drop in specialized flow channel geometries. These models are required for 1-D whole plant transient simulations to be performed for the safety analyses. The present demands of CFD codes make a whole plant CFD simulation impractical. These 1-D models can be obtained in a cost effective manner by the use of geometry correction factors generated

by a CFD code and applied to the results of integral models obtained from experiments in a simpler flow channel geometry (i.e. circular and 1-D).

VIII.   CONCLUSIONS

Several nuclear systems codes are being readied under the Gen IV program as computational tools for conducting performance/safety analyses of the Very High Temperature Reactor. In support of this goal the present project is developing a formal qualification framework, performing an initial filtering of the existing databases, and performing a preliminary screening of tools for use in thermal-hydraulic analyses. The codes are RELAP5/ATHENA for one-dimensional systems modeling and FLUENT and/or Star-CD for three-dimensional modeling.

In year one we developed a methodology for performing this work. We began application of the method by preparing tables of important phenomena in the primary system indexed by operating regime and component. This pre-PIRT process is groundwork for year two when we will develop the actual PIRTs. The mixed convection mode of heat transfer and pressure drop was identified in our work as an important phenomenon for RCCS operation. We focused on the RCCS as a system for demonstration of our methodology. Scaling studies showed that the mixed convection mode is likely to occur in the RCCS air duct during normal operation and during conduction cooldown events. The RELAP5/ATHENA code was found to not adequately treat the mixed convection regime. Readying the code will require adding models for the turbulent mixed convection regime while possibly performing new experiments for the laminar mixed convection regime. Candidate correlations for the turbulent mixed convection regime for the circular channel geometry were identified in the literature. We described the use of computational experiments to obtain correction factors for applying these circular channel results to more specialized channel geometries. The intent is to reduce the number of laboratory experiments. The FLUENT and Star-CD codes contain models that in principle can handle mixed convection but no data were found to indicate that their empirical models for turbulence have been benchmarked for mixed convection conditions. Separate effects experiments were proposed for gathering the needed data.

In years two and three we will move beyond mixed convection in the RCCS to similarly analyze other components and phenomena that are identified as important by the PIRTs. This is consistent with the project objective of identifying weaknesses or gaps in the code models for representing thermal-hydraulic phenomena expected to occur in the VHTR both during normal operation and upsets, identifying the models that need to be developed, and identifying the experiments that must be performed to support model development.

REFERENCES

1.   Gas Turbine-Modular Helium Reactor (GT-MHR) Conceptual Design Report, Report number 910720/1, General Atomics, July 1996.

2.   Philip E. MacDonald et al., *NGNP Point Design—Results of the Initial Neutronics and Thermal-Hydraulic Assessments During FY-03*, INEEL/EXT-03-00870 Rev. 1, Idaho National Engineering and Environmental Laboratory, Idaho Falls, Idaho, September 2003.

3.   B. E. Boyack, et al., "An Overview of Code Scaling, Applicability, and Uncertainty Methodology," Nuclear Engineering and Design 119 (1990), pp. 1-15.

4.   B. Boyack, et al., *Quantifying Reactor Safety Margins, Application of Code Scaling, Applicability, and Uncertainty Evaluation Methodology to Large-Break, Loss-of-Coolant Accident*, NUREG/CR-5249, Nuclear Regulatory Commission, December 1989.

5.   R. B. Vilim, "Designing for a Safe Response to Operational and Severe Accident Initiators in the Integral Fast Reactor," International Topical Meeting on Advanced Reactor Safety, Pittsburgh, PA, pp. 353-364, Vol. 1, (April 1994).

6.   R. Schultz, personal communications, Idaho National Engineering Laboratory, 2004.

7.   P. Hejzlar, personal communications, Massachusetts Institute of Technology, 2004.

8.   P. F. Peterson, "Scaling and Analysis of Mixing in Large Stratified Volumes," Int. J. Heat Mass Transfer, Vol. 37, 1994, Suppl. 1, pp. 97-106.

9.   W. M. Rohsenow and H. Choi, "Heat Mass and Momentum Transfer," Prentice Hall, 1961.

10. B.S. Petukhov, "Heat Transfer in Turbulent Mixed Convection," Hemisphere Publishing, 1988.

11. T. Aicher and H. Martin, New Correlations for mixed turbulent natural and forced convection heat transfer in vertical tubes," International Journal of Heat and Mass Transfer, Vol. 40, No.15, pp. 3617-3626, 1997.

12. W. Williams, P. Hejzlar, M.J. Driscoll, W.J. Lee, and P. Saha, "Analysis of a Convection Loop for GFR Post-LOCA Decay Heat Removal form a Block-Type Core," MIT-ANL-TR-095, March 2003.

13.   F.M. White, *Viscous Fluid Flow*, 2nd ed., Boston: McGraw-Hill, 1991.

14.   IAEA-TECDOC—1382, *Evaluation of high temperature gas cooled reactor performance: Benchmark analysis related to initial testing of the HTTR and HTR-10*, Chapter 3, "High Temperature Engineering Test Reactor Thermal Hydraulic Benchmarks, November 2003.

15.   IAEA-TECDOC—1163, *Heat Transport and Afterheat Removal for Gas Cooled Reactors under Accident Conditions*, 2000.

16.   T. Krauss and L. Meyer, "Experimental investigation of turbulent transport of momentum and energy in a heated rod bundle", *Nuclear Engineering and Design, 180, pp. 185-206 (1998).*

17.   K. Kunitomi, "Thermal and Hydraulic Tests in HENDEL T_2 Supporting the Development of the Core Bottom Structure of the High Temperature Engineering Test Reactor (HTTR)," *Nuclear Engineering and Design*, Vol. 108, 1988, pp. 359-368.

18.   Yoshiaki Miyamoto, et al., "Thermal and Hydraulic Test of Test Sections in the Helium Engineering Demonstration Loop," *Nuclear Engineering and Design*, Vol. 120, 1990, pp. 435-445.

19.   Yoshiyuki Inagaki, et al., "Thermal-Hydraulic Characteristics of Coolant in the Core Bottom Structure of the High-Temperature Engineering Test Reactor," *Nuclear Technology*, Vol. 99, July 1992, pp. 90-103.

20.   Yoshiyuki Inagaki, Tomoaki Kunugi, and Yoshiaki Miyamoto, "Thermal Mixing Test of Coolant in the Core Bottom Structure of a High Temperature Engineering Test Reactor," *Nuclear Engineering and Design*, Vol. 123, 1990, pp. 77-86.

21.   Makoto Hishida, et al., "Heat Transfer Problems in a VHTR," *Heat Transfer in High Technology and Power Engineering*, Wen-Jei Yang and Yasuo Mori, editors, Hemisphere Publishing Corporation, New York, 1987, pp. 273-284.

22.   M. S. Yao, Z. Y. Huang, C. W. Ma, and Y. H. Xu, "Simulating Test for Thermal Mixing in the Hot Gas Chamber of the HTR-10," *Nuclear Engineering and Design*, Vol. 218, 2002, pp. 233-240.

23.   G. Damm and R.Wehrlein, "Simulation Tests for Temperature Mixing in a Core Bottom Model of the HTR-Module," *Nuclear Engineering and Design*, Vol. 137, 1992, pp. 97-105.

APPENDIX A Bibliography by Subject

Analysis and Experimental Needs of Generation IV Reactors

1.   T. A. Taiwo and H. S. Khalil, *Assessment of Analysis Capabilities for Generation IV System Design*, Nuclear Engineering Division, Argonne National Laboratory, September 23, 2003.

2.   Minutes of Workshop on Thermal-Hydraulic and Safety Analysis Tools for Generation IV Nuclear Energy Systems, Idaho National Engineering and Environmental Laboratory, Idaho Falls, Idaho, March 18-19, 2003.

3.   L. J. Siefken, E. A. Harvego, E. W. Coryell, and C. B. Davis, "Transient Analysis Needs for Generation IV Reactor Concepts," Proceedings of 10th International Conference on Nuclear Energy, Arlington, VA, April 14-18, 2002, ICONE10-22641, pp. 1-18.

4.   Donald M. McEligot, et al., "Thermalhydraulics Studies for Improved Safety and Efficiency of Gas-Cooled Fast-Breeder Reactors (GFRs) and Advanced HTGRs," Nuclear Energy Research Initiative Proposal Program Announcement LAB-NE-2002-1, submitted April 17, 2002.

5.   Email from Khalil to Taiwo, January 7, 2004, with INEEL work package on NGNP "design and evaluation methods" mentioned and scope of work to be done briefly described.

6.   Finis H. Southworth, "Very High Temperature Gas Cooled Reactor System (VHTR, Thermal-Hydraulic Analyses and Assessment Needs," slide presentation, Thermal-Hydraulic and Safety Analysis Tools for Generation IV Nuclear Energy Systems, Idaho National Engineering and Environmental Laboratory, Idaho Falls, Idaho, March 18-19, 2003.

7.   Richard R. Schultz, Walter L. Weaver, Abderrafi M. Ougouag, and William A. Wieselquist, "Validating & Verifying a New Thermal-Hydraulic Analysis Tool," Proceedings of 10th International Conference on Nuclear Energy, Arlington, VA, April 14-18, 2002, ICONE10-22446, pp. 1-8.

8.   Donald M. McEligot, et al., "Fundamental Thermal Fluid Physics of High Temperature Flows in Advanced Reactor Systems," INEEL/EXT-2002-1613, Nuclear Energy Research Initiative, Final Report, Project No. 99-254, Reporting Period: (September 1999-October 2002), December 31, 2002.

VHTR and GT-MHR

9.   Paul D. Bayless, "VHTR Thermal-Hydraulic Scoping Analysis Using RELAP55-3D/ATHENA," Global 2003, New Orleans, LA, November 16-20, 2003.

10. Philip E. MacDonald et al., *NGNP Point Design—Results of the Initial Neutronics and Thermal-Hydraulic Assessments During FY-03*, INEEL/EXT-03-00870 Rev. 1, Idaho National Engineering and Environmental Laboratory, Idaho Falls, Idaho, September 2003.

11. Finis Southworth, Franck Carre, and Philip Hildebrandt, "Generation IV Gas Cooled Reactor Concepts," *Transactions of the American Nuclear Socie*ty, Vol. 85, November 11-15, 2001, Reno, Nevada, pp. 66-67.

12. *Gas Turbine-Modular Helium Reactor (GT-MHR) Conceptual Design Description Report*, 910720, Revision 1, GA Project No. 7658, General Atomics, July 1996.

13. M. P. La Bar and W. A. Simon, "International Cooperation in Developing the GT-MHR," Technical Committee Meeting on High Temperature Gas Cooled Reactor Technology Development, IAEA-TECDOC—988, Johannesburg, South Africa, November 13-15, 1996.

14. J. H. Gittus, "The ESKOM Pebble Bed Modular Reactor," *Nuclear Energy*, Vol. 38, No. 4, August 1999, pp. 215-221.

HTGR and MHTGR

15. *Proceedings of the Third Japan—U.S. Seminar on HTGR Safety Technology,* NUREG/CP-0045, BNL-NUREG-51674, Vol. 1, Brookhaven National Laboratory, June 2-3, 1982. (See in particular, S. Mitake, et al., "Study of the Experimental VHTR Safety with Analysis for a Hypothetical Rapid Depressurization Accident," pp. 117-129.)

16. P. M. Williams, T. L. King, and J. N. Wilson, *Draft Preparation Safety Evaluation Report for the Modular High-Temperature Gas-Cooled Reactor*, NUREG-1338, March 1989.

17. DOE, *Evaluation of the Gas Turbine Modular Helium Reactor*, DOE-GT-MHR-100002, February 1994.

Specific Codes

18. Syd Ball, "The ORNL 'GRSAC' Code for Gas Reactor Simulation – Thermal Hydraulics, and Severe Accidents," slide presentation, Gen-4 T/H Workshop – INEEL, March 18-19, 2003, Idaho Falls, Idaho.

19. Richard R. Schultz, Richard A. Riemke, Cliff B. Davis, and Greg Nurnberg, "Comparison: RELAP55-3D[©] Systems Analysis Code & Fluent CFD Code Momentum Equation Formulations," Proceedings of 11th International Conference on Nuclear Energy, Tokyo, Japan, April 20-23, 2003, ICONE11-36585., pp. 1-9.

20.	Richard R. Schultz and Walter L. Weaver, "Using the RELAP55-3D[©] Advanced Systems Analysis Code with Commercial and Advanced CFD Software," Proceedings of 11th International Conference on Nuclear Energy, Tokyo, Japan, April 20-23, 2003, ICONE11-36545, pp. 1-7.

21.	Gary Johnsen and Cliff Davis, "RELAP55-3D/ATHENA Capabilities for Analyzing Generation IV Reactors," slide presentation, Thermal-Hydraulic and Safety Analysis Tools for Generation IV Nuclear Energy Systems, Idaho National Engineering and Environmental Laboratory, Idaho Falls, Idaho, March 18-19, 2003.

22.	K. Fischer, H. Holzbauer, and L. Wolf, "Battelle-Europe Verifications and Extensions of the Gothic Code," *Proceedings of the Fifth International Topical Meeting of Reactor Thermal Hydraulics*, NURETH-5, sponsored by the Thermal Hydraulics Division of and Idaho Section of the American Nuclear Society, September 21-24, 1992, Little America Hotel, Salt Lake City, UT, USA.

Reactor Cavity Cooling System

23.	*450 MWt Reactor Cavity Cooling System System Design Description*, DOE-HTGR-90016, Revision 0, Bechtel National, Inc., November 1993.

24.	J. C. Conklin, *Modeling and Performance of the MHTGR Reactor Cavity Cooling System*, NUREG/CR-5514, ORNL/TM-11451, R1, R7, R8, April 1990.

25.	A. Woaye-Hune and S. Ehster, "Calculation of Decay Heat Removal Transient by Passive Means for a Direct Cycle Modular HTR," *Proceedings of the Conference on High Temperature Reactors*, Petten, NL, April 22-24, 2002.

Experiments in HDR Facility (Hydrogen Distribution in LWR)

26.	Luis A. Valencia, "Hydrogen Distribution Test Under Severe Accident Conditions at the Large-Scale HDR-Facility," *Nuclear Engineering and Design*, Vol. 140, (1993), pp. 51-60.

27.	P. N. Smith and P. Ellicott, "A UK Analysis of Light Gas Distribution Experiment E11.2 in the HDR Facility," *Nuclear Engineering and Design*, Vol. 140, (1993), pp. 61-68.

28.	I. M. Coe and D. B. Utton, "The Use of the COMPACT Code for Calculation of Long Term Environmental Effects as a Result of High Temperature Discharges into Confined Areas," *Nuclear Engineering and Design*, Vol. 140, (1993), pp. 69-78.

Scaling of Large Stratified Volumes

29.	P. F. Peterson, "Scaling and Analysis of Mixing in Large Stratified Volumes," Int. J. Heat Mass Transfer, Vol. 37, 1994, Suppl. 1, pp. 97-106.

30.   P. F. Peterson, V. E. Schrock, R. Greif, "Scaling for Integral Simulation of Mixing in Large, Stratified Volumes," *Nuclear Engineering and Design*, Vol. 186, 1998, pp. 213-224.

31.   ANL Intra-Laboratory Memo, W. A. Bezalla to T. Y. C. Wei, "Scaling Considerations of BMC Experiments," November 1, 1995.

32.   ANL Intra-Laboratory Memo, Y. W. Shin to T. Y. C. Wei, "Scaling and Similitude Studies of HDR Tests and SBWR Reference Accidents," November 2, 1995.

Code Scaling, Applicability, and Uncertainty Methodology
33.   B. Boyack, et al., *Quantifying Reactor Safety Margins, Application of Code Scaling, Applicability, and Uncertainty Evaluation Methodology to Large-Break, Loss-of-Coolant Accident*, NUREG/CR-5249, Nuclear Regulatory Commission, December 1989.

34.   B. E. Boyack, et al., "An Overview of Code Scaling, Applicability, and Uncertainty Methodology," Nuclear Engineering and Design 119 (1990), pp. 1-15.

35.   G. E. Wilson, et al., "Characterization of Important Contributors to Uncertainty," Nuclear Engineering and Design 119 (1990), pp. 17-31.

36.   W. Wulff, et al., "Assessment and Ranging of Parameters," Nuclear Engineering and Design 119 (1990), pp. 33-65.

37.   G. S. Lellouche, et al., "Uncertainty Evaluation of LBLOCA Analysis Based on TRAC-PF1/MOD 1," Nuclear Engineering and Design 119 (1990), pp. 67-95.

38.   N. Zuber, et al., "Evaluation of Scale-Up Capabilities of Best Estimate Codes," *Nuclear Engineering and Design* 119 (1990), pp. 97-107.

39.   I. Catton, et al., "A Physically Based Method of Estimating PWR Large Break Loss of Coolant Accident PCT," *Nuclear Engineering and Design* 119 (1990), pp. 109-117.

40.   F. F. Cadek, L. E. Hochreiter, and M. Y. Young, Best Estimate Approach for Effective Plant Operation and Improved Economy, Electric Power Research Institute Workshop on Appendix "K" Relief Using Best Estimate Methods: The Revised LOCA/ECCS Rule, Cambridge, Massachusetts (August 11-12, 1988).

41.   Andrej Prosek and Borut Mavko, "Evaluting Code Uncertainty-I: Using The CSAU Method for Uncertainty Analysis of a Two-Loop PWR SBLOCA," *Nuclear Technology*, Vol. 126, May 1999.

42. *An Integrated Structure and Scaling Methodology for Severe Accident Technical Issue Resolution*, NUREG/CR-5809, EGG-2659, R4, November 1991.

Phenomena Identification and Ranking Table and Analytical Hierarchy Process
43. R. A. Shaw, et al., *Development of a Phenomena Identification and Ranking Table (PIRT) for Thermal-Hydraulic Phenomena During a PWR Large-Break LOCA*, NUREG/CR-5074, EGG-2527, R4, Idaho National Engineering Laboratory, November 1988.

44. T. Saaty, *Decision-making For Leaders*, Belmont California, Lifetime Learning Publications, Wadsworth Inc., 1982.

45. Thomas L. Saaty and Kevin P. Kearns, *Analytical Planning, The Organization of Systems*, Pergamon Press, New York, 1985.

46. Thomas L. Saaty, *The Analytical Hierarchy Process*, McGraw-Hill, New York, 1980.

Thermal Striping and Fluctuations Due to Mixing
47. E. E. Feldman, L. K. Chang, and M. J. Lee, "Thermal Striping of Rod— Thermoelastic Solutions for Sinusoidal Fluid Temperatures," ASME Pressure Vessel Conference, San Diego, California, June 23-27, 1991.

48. M. J. Lee, L. K. Chang, and E. E. Feldman, "Plastic Analysis of A Circular Rod Subjected to Sinusoidal Thermal Cycling," ASME Pressure Vessel Conference, San Diego, California, June 23-27, 1991.

49. A. Nordgren, "Thermal Fluctuations in Mixing Tees (Experiences, Measurements, Predictions and Fixes)," *Transactions of the 7th International Conference on Structural Mechanics in Reactor Technology*, 1983, Vol . D. , pp. 7-14.

Materials and Material Codes
50. Bill Corwin, "Materials for Gen IV Reactors," slides presentation, UNLV Workshop on High-Temperature Heat Exchangers, Las Vegas, April 17, 2003.

51. K. Natesan, A,. Purohit, and S. W. Tam, *Material Behavior in HTGR Environments*, NUREG/CR-6824, ANL-02/37, by ANL for US NRC, July 2003.

52. V. N. Shah, S. Majumdar, and K. Natesan, *Review and Assessment of Codes and Procedures for HTGR Components*, NUREG/CP-6816, ANL-02/36, by ANL for US NRC, June 2003.

Experimental Data from Gas Reactor and Component Mockups
53. Makoto Hishida, et al., "Heat Transfer Problems in a VHTR," *Heat Transfer in High Technology and Power Engineering*, Wen-Jei Yang and Yasuo Mori, editors, Hemisphere Publishing Corporation, New York, 1987, pp. 273-284.

54.   IAEA-TECDOC—1382, *Evaluation of high temperature gas cooled reactor performance: Benchmark analysis related to initial testing of the HTTR and HTR-10*, Chapter 3, "High Temperature Engineering Test Reactor Thermal Hydraulic Benchmarks", 2000.

55.   Y. Shiina and M. Hishida, "Heat Transfer in the Upper Part of the HTTR Pressure Vessel During Loss of Forced Cooling," Specialists Meeting on Decay Heat Removal and Heat Transfer Under Normal and Accident Conditions in Gas Cooled Reactors, IAEA-TECDOC—757, Juelich, Germany, July 6-8, 1992, pp. 125-130.

56.   IAEA-TECDOC—1163, *Heat Transport and Afterheat Removal for Gas Cooled Reactors under Accident Conditions*.

57.   Yoshiaki Miyamoto, et al., "Thermal and Hydraulic Test of Test Sections in the Helium Engineering Demonstration Loop," *Nuclear Engineering and Design*, Vol. 120, 1990, pp. 435-445.

Air Ingress

58.   Motoo Fumizawa, et al., "Numerical Analysis of Buoyancy-Driven Exchange Flow with Regard to an HTTR Air Ingress Accident," *Nuclear Technology*, Vol. 110, May 1995, pp. 263-272.

59.   M. Hishida, et al., "Research on Air Ingress Accidents of the HTTR," *Nuclear Engineering and Design*, Vol. 144, 1993, pp. 317-325.

Commercial CFD Codes in General

60.   C. J. Freitas, "Perspective: Selected Benchmarks from Commercial CFD Codes," *Transactions of the ASME, Journal of Fluid Mechanics*, Vol. 117, June 1995, pp. 208-218.

Outlet Plenum

61.   N. Tauveron, "Thermal Fluctuations in the Lower Plenum of an High Temperature Reactor," *Nuclear Engineering and Design*, Vol. 222, 2003, pp. 125-137.

62.   G. Damm and R.Wehrlein, "Simulation Tests for Temperature Mixing in a Core Bottom Model of the HTR-Module," *Nuclear Engineering and Design*, Vol. 137, 1992, pp. 97-105.

63.   Yoshiyuki Inagaki, Tomoaki Kunugi, and Yoshiaki Miyamoto, "Thermal Mixing Test of Coolant in the Core Bottom Structure of a High Temperature Engineering Test Reactor," *Nuclear Engineering and Design*, Vol. 123, 1990, pp. 77-86.

64.   K. Kunitomi, "Thermal and Hydraulic Tests in HENDEL T_2 Supporting the Development of the Core Bottom Structure of the High Temperature Engineering Test Reactor (HTTR)," *Nuclear Engineering and Design*, Vol. 108, 1988, pp. 359-368.

65.   M. S. Yao, Z. Y. Huang, C. W. Ma, and Y. H. Xu, "Simulating Test for Thermal Mixing in the Hot Gas Chamber of the HTR-10," *Nuclear Engineering and Design*, Vol. 218, 2002, pp. 233-240.

66.   Yoshiyuki Inagaki, et al., "Thermal-Hydraulic Characteristics of Coolant in the Core Bottom Structure of the High-Temperature Engineering Test Reactor," *Nuclear Technology*, Vol. 99, July 1992, pp. 90-103.

67.   N. Tauveron, M. Elmo, O. Cionti, T. Chataing, "Thermal Hydraulic Simulations of High Temperature Reactors", *Proceedings of the Conference on High Temperature Reactors*, Petten, NL, April 22-24, 2002.

<u>Natural, Mixed, and Forced Convection</u>

68.   G. Fu, "Heat Transfer and Friction Factor Behavior in the Mixed Convection Regime for Air Up-Flow in a Heated Vertical Pipe," Heat Transfer—Minneapolis 1991, AIChe Symposium Series, Vol. 87, No. 283, American Institute of Chemical Engineers, New York, 1991, pp. 326-335.

69.   G. Fu, N. E. Todreas, P. Hejzlar, and M. J. Driscoll, "Heat Transfer Correlation for Reactor Riser in Mixed Convection Air Flow," *Transactions of the ASME, Journal of Heat Transfer*, Vol. 116, May 1994, pp. 489-492.

70.   Wesley Williams, Pavel Hejzlar, Michael Driscoll, Won Jae Lee, and Pradip Saha, *Analysis of a Convection Loop for GFR Post-LOCA Decay Heat Removal from a Block-Type Core*, MIT-ANP-TR-095, Program for Advanced Nuclear Power Studies, Nuclear Engineering Department, Massachusetts Institute of Technology, Cambridge, MA.

71.   Sadik Kakaç, Ramesh K. Shak, and Win Aung, *Handbook of Single-Phase Convective Heat Transfer*, John Wiley and Sons, New York, 1987.

72.   Simon Ostrach, "Natural Convection Heat Transfer in Cavities and Cells," *Heat Transfer 1982, Proceedings of the Seventh International Heat Transfer Conference*, München, Fed. Rep. of Germany, Ed. U. Grigull, et al., Hemisphere Publishing Corporation, New York, 1982, pp.365-379.

APPENDIX B Outlet Plenum Experiments

Similarly to the database screening work reported in Section VII some initial work was also performed on screening experiments for the outlet plenum mixing phenomena. This work is documented here. Table B.1 identifies the experiments while Table B.2 shows the range of conditions and important nondimensional parameters for these experiments. The references shown in Table B.1 are identified in the section References.
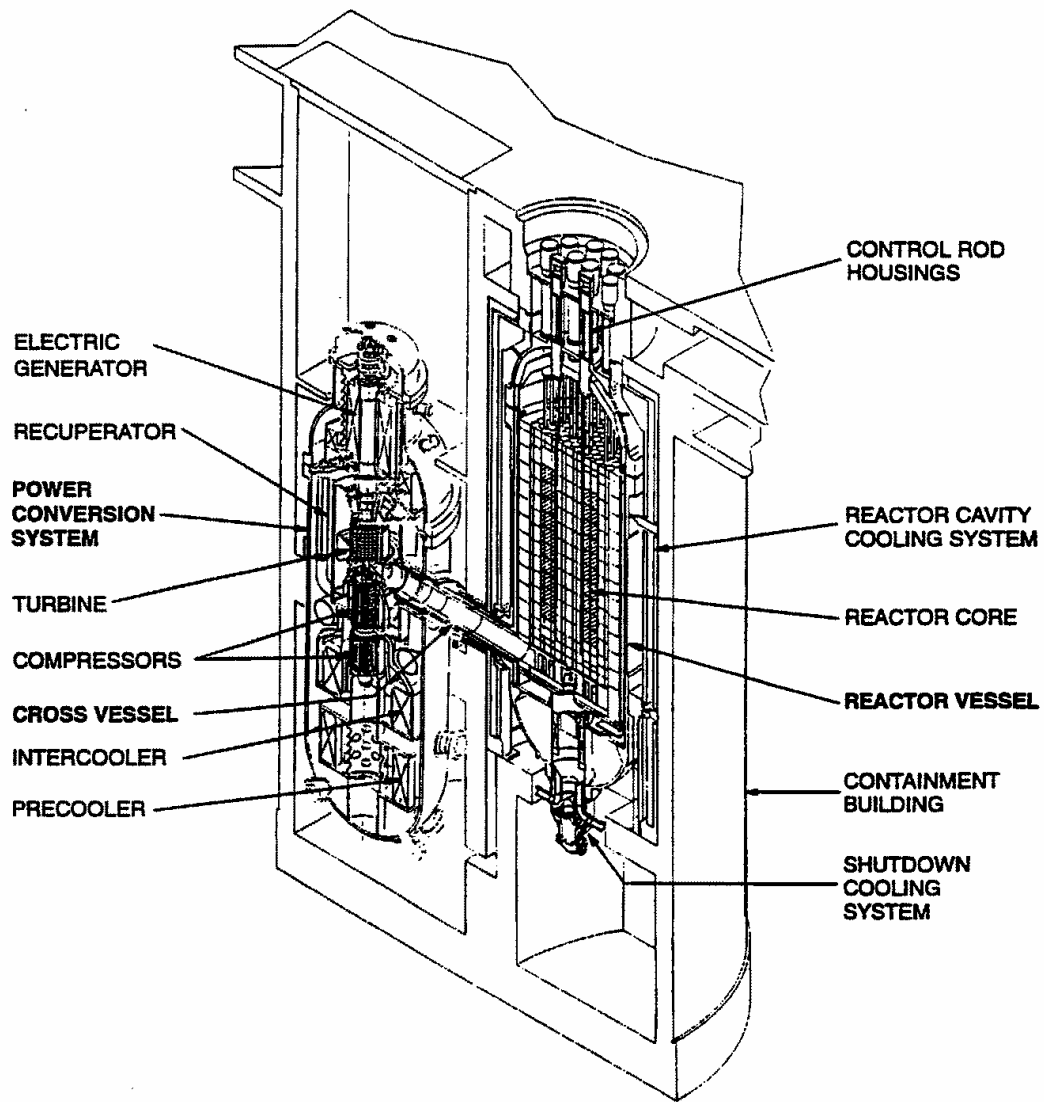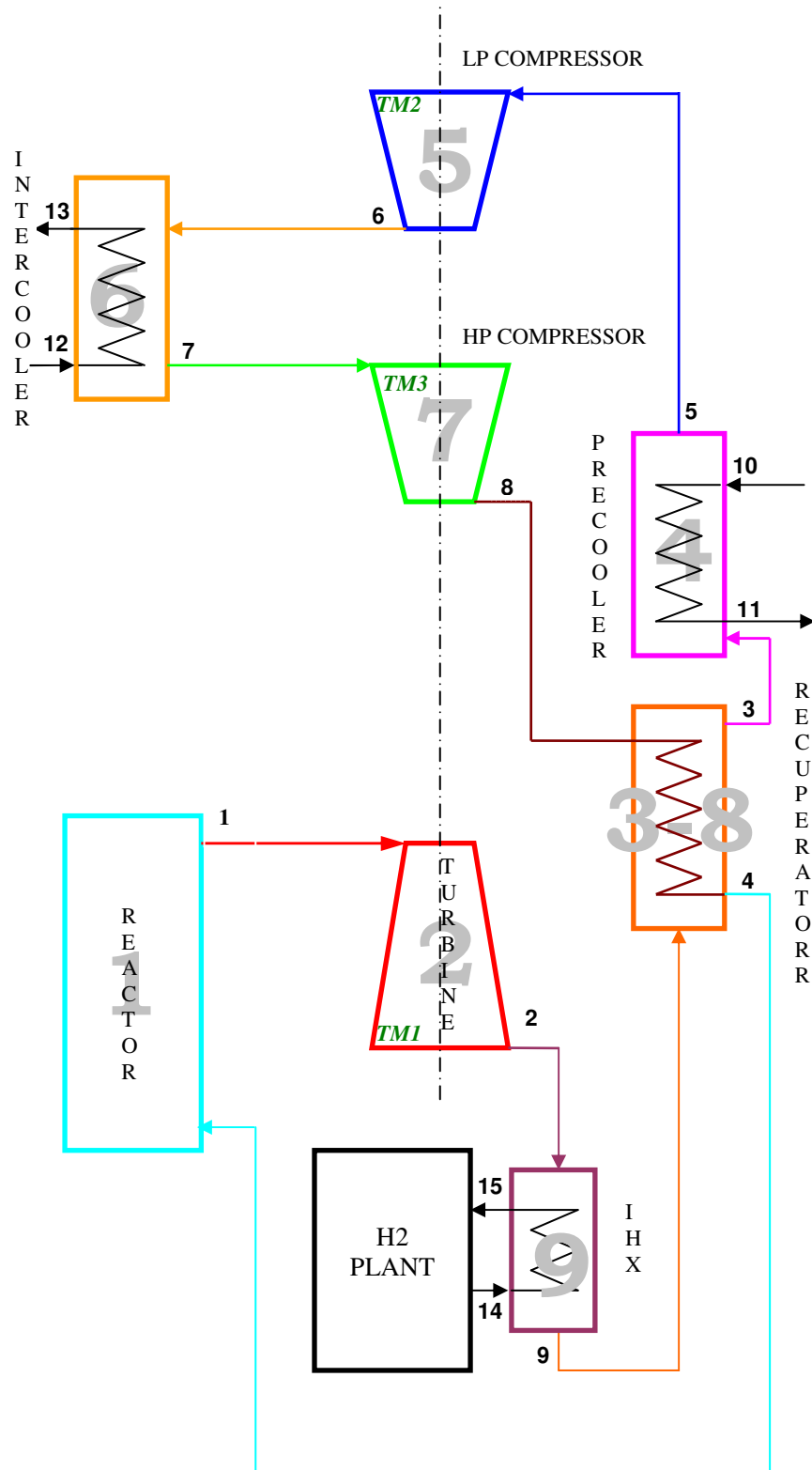
Fig. 1 Isometric View of the NGNP [1]

Fig. 2 Schematic of Main Components of the NGNP
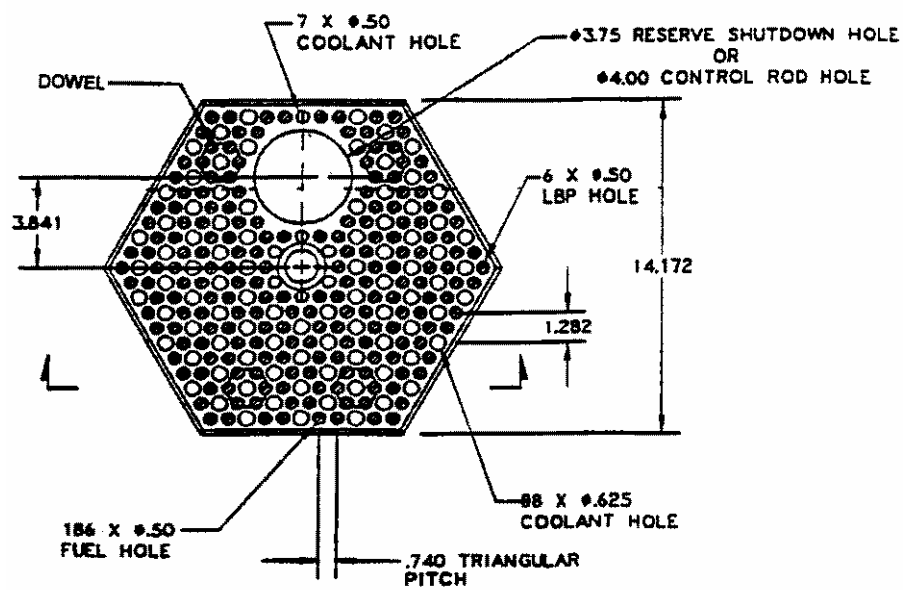
Fig. 3 Top View of a Fuel Element for the Prismatic Core [1]
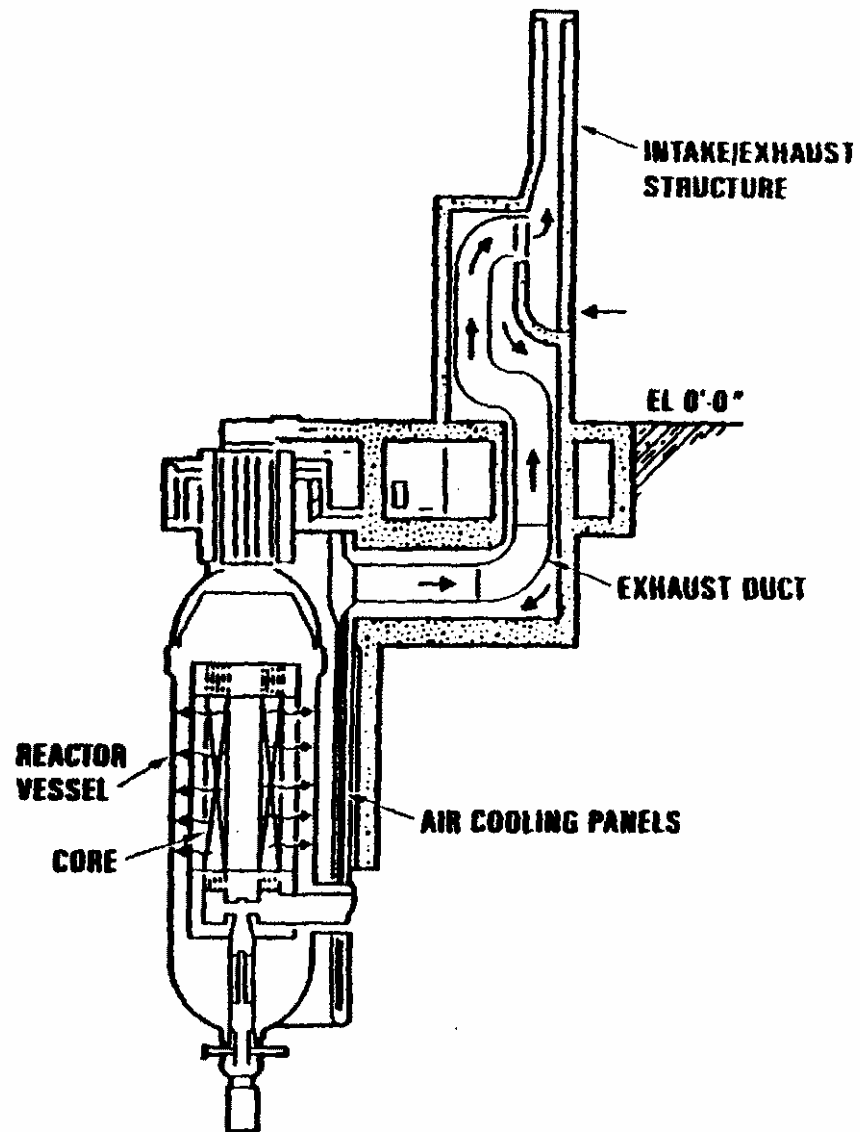
Fig. 4 Schematic of the RCCS [1]
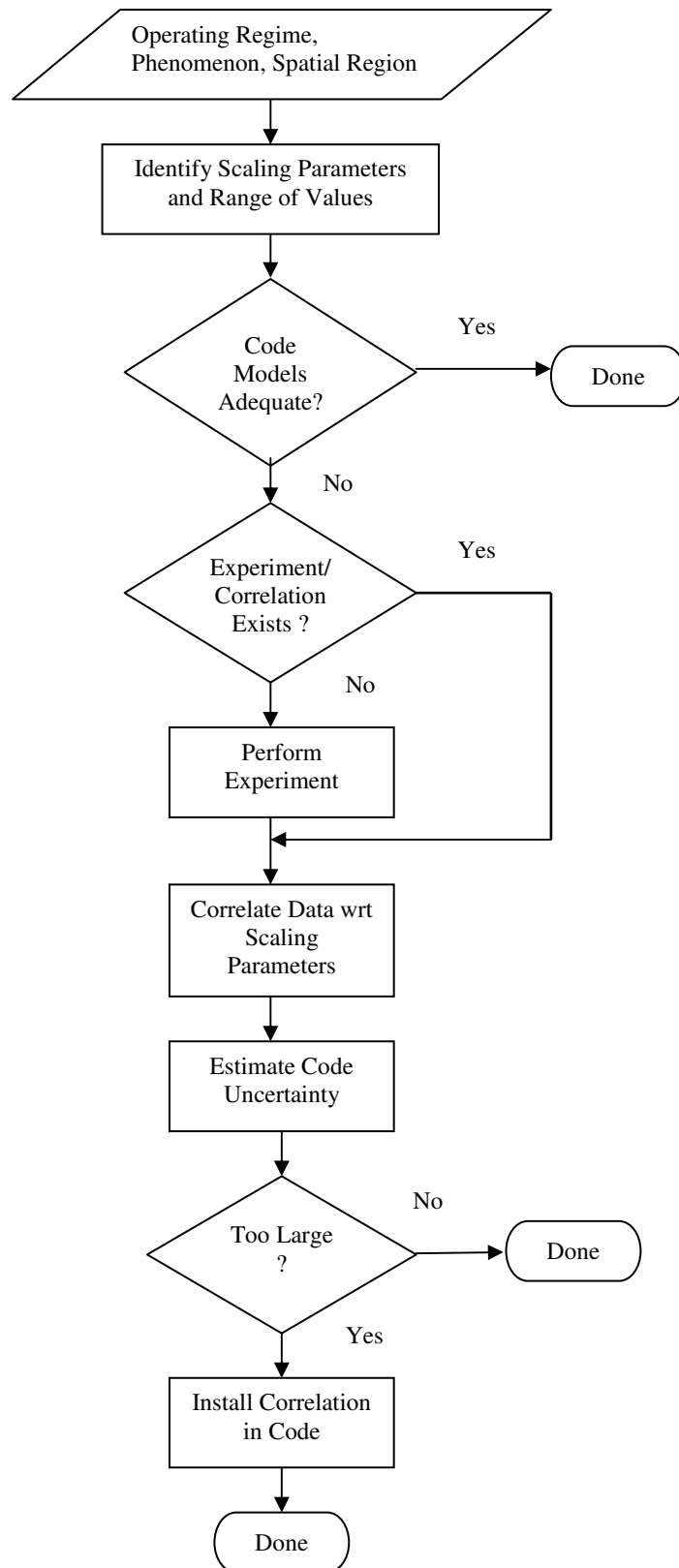
Fig. 5 Code Evaluation/Improvement Process

Design Basis
Events

Phenomena

Component

Operating
Regime

Material
Limit
(basis for
Safety
Criteria)

Specific Safety Issue
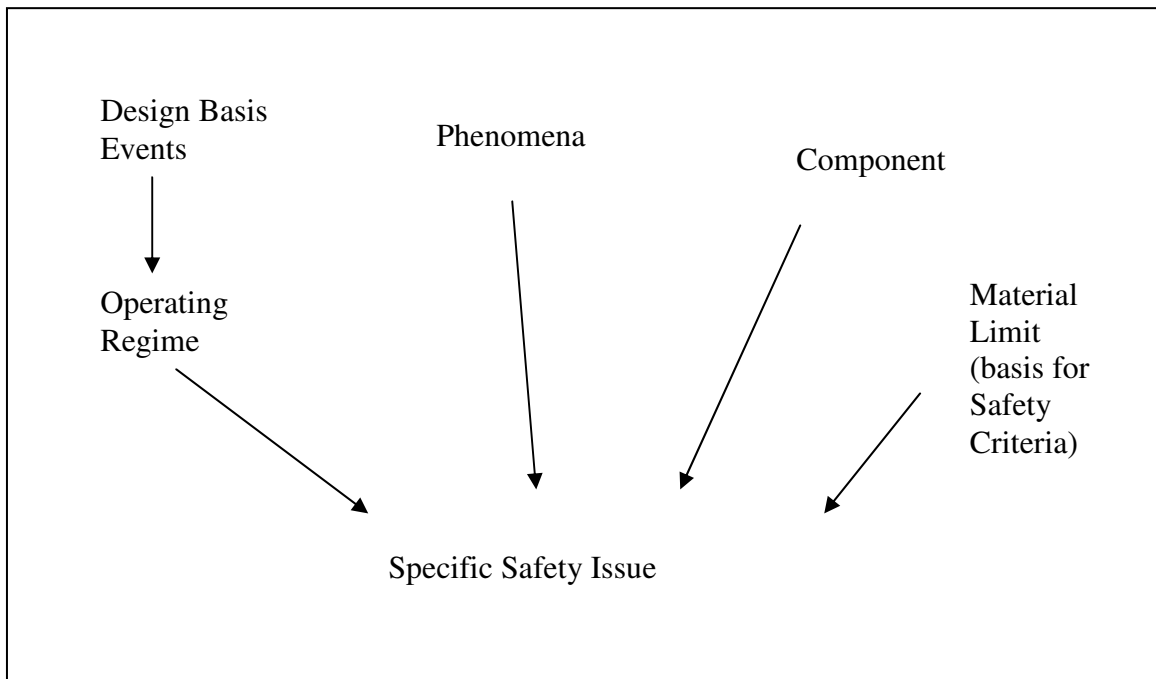
Fig. 6 Factors Giving Rise to Safety Issues

Thermal Hydraulic Operating Regime =

f (Pressure, Cooling Mode, Heating Mode)

- Normal
- Depressurized

- Forced Convection Cooling (PCU or Shutdown Cooler driven with net flow through reactor core)
- Conduction Cooling (RCCS driven with no net flow through reactor core)

- Neutronic Power
- Shutdown Decay Power
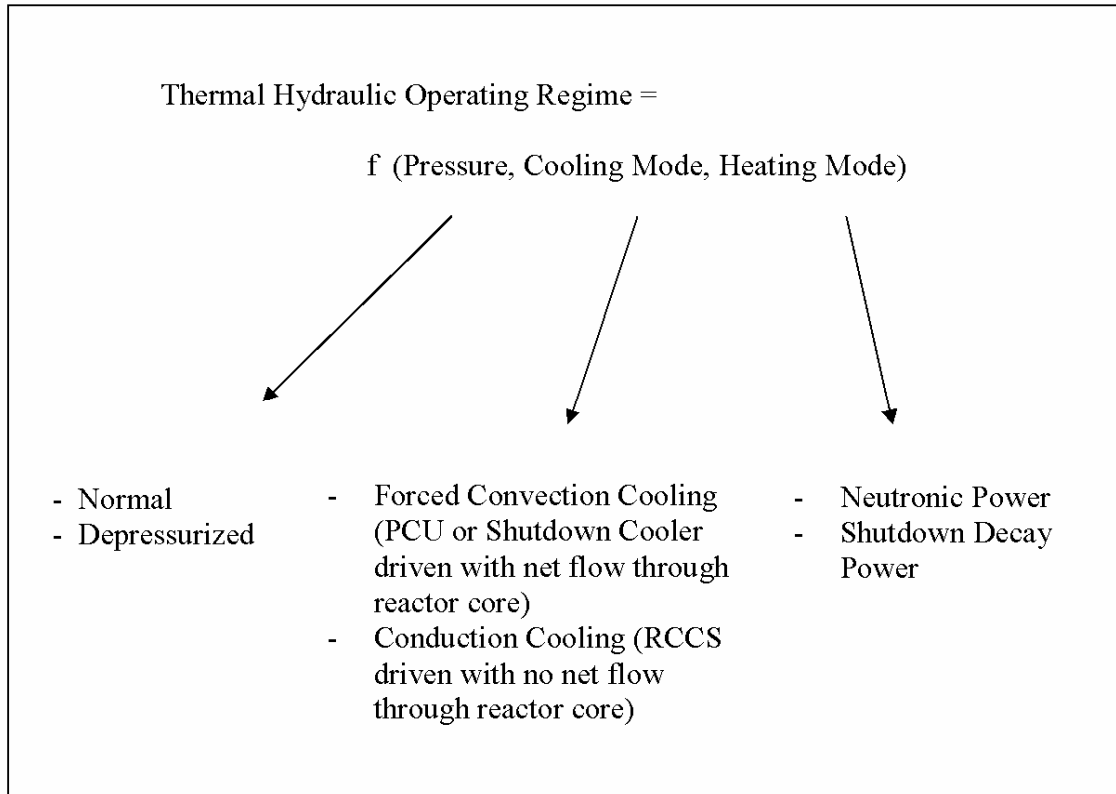
Fig. 7 Factors Influencing Thermal-Hydraulic Operating Regime
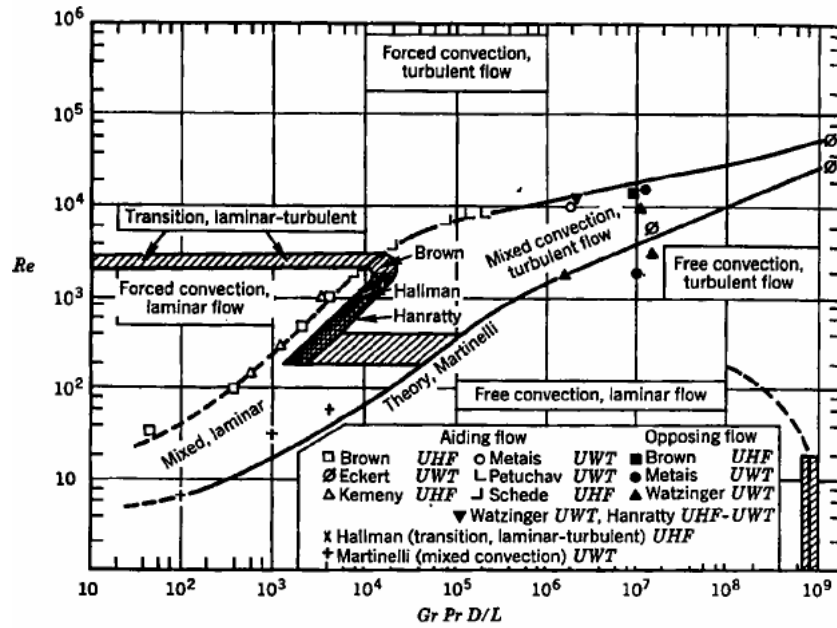
Fig. 8 Map Identifying Mixed Convection Regime [12]
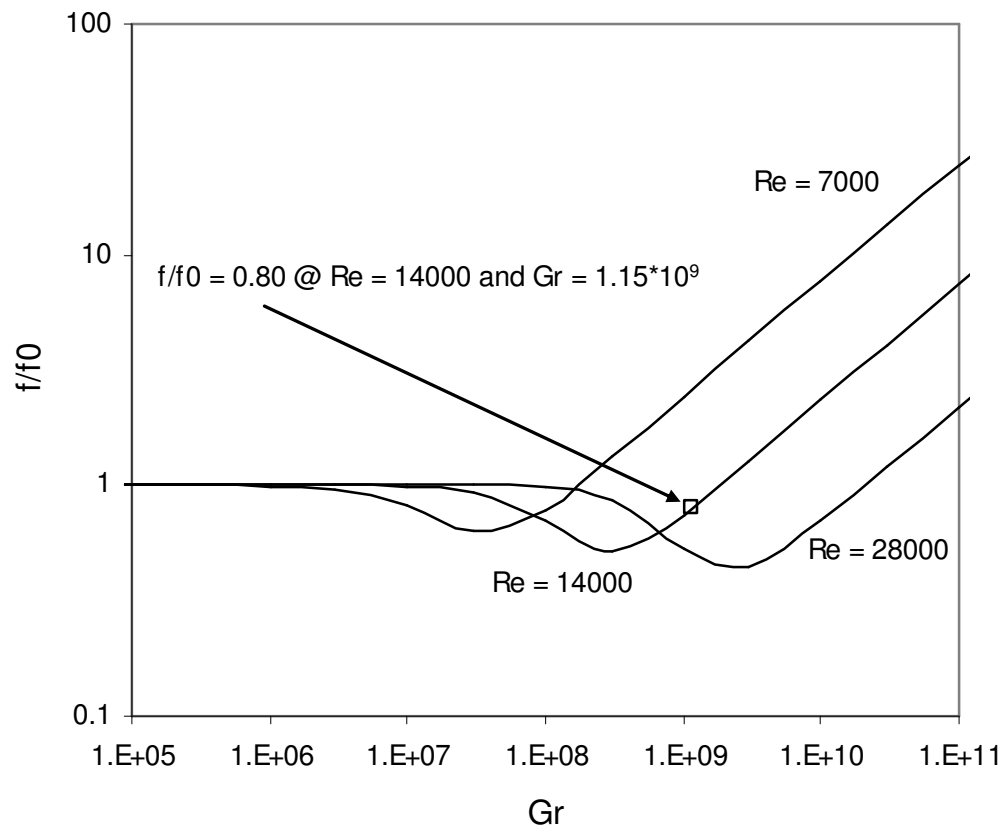
Fig. 9 Ratio of Friction Factor in Vertical Upflow Heated Pipe to that in Unheated Pipe
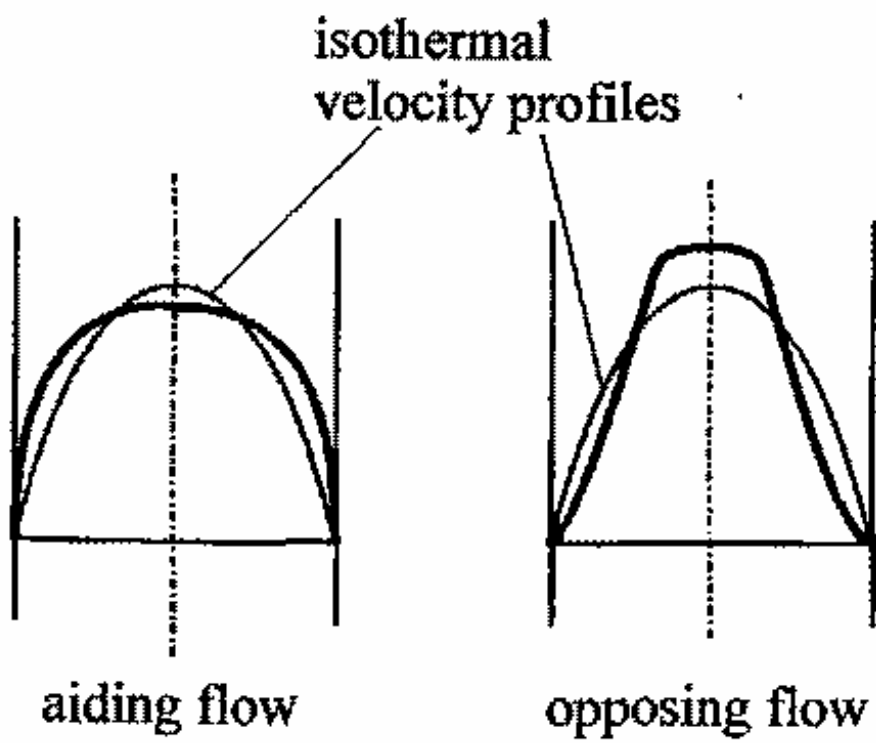
Fig. 10 Velocity Profiles under Aiding and Opposing Turbulent Flow Conditions [11]
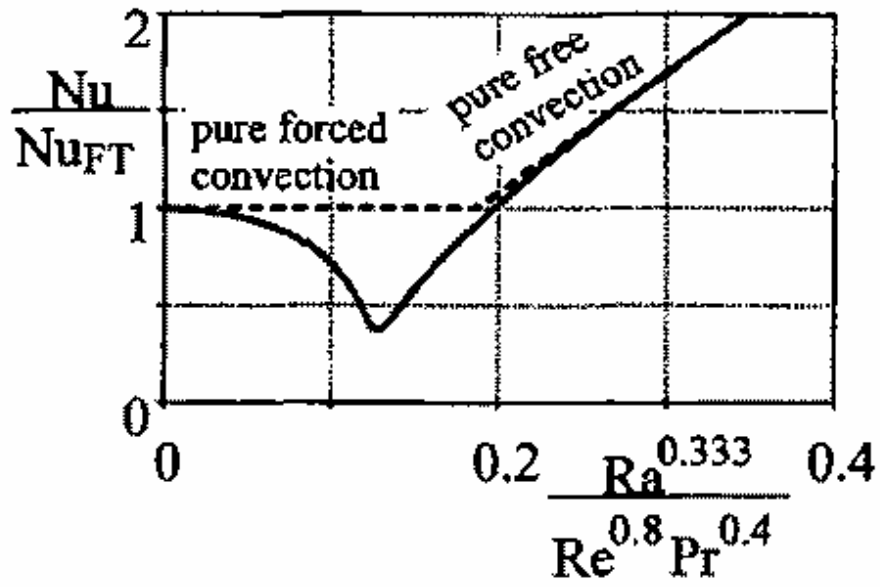
Fig. 11 Heat Transfer for Aiding Mixed Convection [11]

Table I Fuel Element Coolant Channel Dimensions and Full Power Thermal-Hydraulic Conditions

Parameter	Value
Reactor Power, Q (Mwt)	600
Reactor Mass Flowrate , W (kg/s)	320
Coolant Channel Diameter, D (m)	0.0159
Flow Fraction to Fuel Elements	0.8
Number of Fuel Element Columns, n_c	102
Number of Coolant Channels per Fuel Element, n_h	108
Length of Active Core Coolant Channel, L (m)	7.93
Average Fuel Element Coolant Channel Flowrate , w (kg/s)	0.023
Coolant Channel Wall Heat Flux, (Mw/m^2) $q'' = Q/(n_c n_h \pi DL)$	0.137

Table II RCCS Duct Dimensions and Thermal-Hydraulic Conditions at Reactor Full Power

Parameter	Value
RCCS Power*, Q (Mwt)	3.3
RCCS Air Mass Flowrate *, W (kg/s)	14.3
Number of Ducts*, n	292
Average Duct Air Flowrate , w (kg/s)	0.049
Duct Dimensions*, a=horizontal width of heat transfer surface x b=horizontal depth (m)	0.05 x 0.25
Hydraulic Diameter, D (m)	0.083
Length of Active Core Region, L (m)	7.93
Duct Wall Heat Flux, (Mw/m^2) $q'' = Q/(naL)$	0.029

 * from [1].

Table III Relationship of Duty Cycle/Design Basis Events to Features of Asymptotic Steady-State Operating Regime

| | | | Full Power Operation | Operational Transients | Refueling | Upsets | | | | | | | | | | | | | | |
| | | | | | | Protected | | | | | | | Unprotected | | | | | | |
						Loss of Generator Load	Reactivity Insertion	Loss of Cooling	Shaft Breakage	Loss of Coolant	Overcooling	Flow Blockage	Loss of Generator Load	Reactivity Insertion	Loss of Cooling	Shaft Breakage	Loss of Coolant	Overcooling	Flow Blockage
Values of Operating Regime Variables	Pressure	Normal Pressure	X	X		X	X	X	X		X	X	X	X	X	X		X	X
		Depressurized			X					X							X		
	Cooling	Forced Convection	X	X	X	X	X		X		X		X	X		X		X	
		Conduction						X		X		X				X	X		X
	Heating	Neutronic	X	X									X	X	X	X	X	X	X
		Decay Heat			X	X	X	X	X	X	X	X							

Table IV Asymptotic Steady-State Operating Regimes and the Duty Cycle/Design Basis
Events They Encompass. Ranked Generally in Order of Increasing Severity

Asymptotic Steady-State Operating Regime	Initiating Duty Cycle/Design Basis Events
OR1 - Normal Pressure/ Forced Convection Cooling/ Shutdown Decay Heat Generation	Loss of Generator Load - Protected Reactivity Insertion – Protected Shaft Breakage – Protected Overcooling - Protected
OR2 - Normal Pressure/ Forced Convection Cooling/ Neutronic Power	Full Power Operation. Operational Transients. Loss of Generator Load - Unprotected Reactivity Insertion – Unprotected Shaft Breakage – Unprotected Unprotected Overcooling - Unprotected
OR3 - Normal Pressure/ Conduction Cooling/ Shutdown Decay Heat	Loss of Cooling - Protected Flow Blockage - Protected
OR4 - Normal Pressure/ Conduction Cooling/ Neutronic Power	Loss of Cooling - Unprotected Flow Blockage - Unprotected
OR5 - Depressurized/ Forced Convection Cooling/ Shutdown Decay Heat	Refueling
OR6 - Depressurized/ Conduction Cooling/ Shutdown Decay Heat	Loss of Coolant - Protected
OR7 - Depressurized/ Conduction Cooling/ Neutronic Power	Loss of Coolant - Unprotected

Table V List of Phenomena and Potential Safety Issues

Phenomena	Issue
P1. Thermal Stratification in a Plenum	Poor mixing may hinder heat removal resulting in elevated temperatures and material creep.
P2. Jet Discharging Into a Plenum	a. Induced spatial and temporal variations in temperature of the plenum wall may result in material fatigue. b. Momentum of impinging stream may damage insulation.
P3. Laminar-Turbulent Transition Flow	Models must accurately represent pressure drop and heat transfer rate to ensure design flowrates are adequate for required heat removal rate.
P4. Forced-Natural Mixed Convection Flow	Models must accurately represent pressure drop and heat transfer rate to ensure design flowrates are adequate for required heat removal rate.
P5. Radiant Heat Transfer	Prediction of radiant heat transfer in complex geometries is difficult potentially leading to under-prediction of cooling.
P6. Spatially Non-Uniform Heat Flow in Thick-Walled Structure at Steady State	Large spatial temperature gradients can lead to large thermal stress and component fatigue. Mixing junctions are vulnerable.
P7. Temperature Profile in Thick-Walled Structure During Transient	Large temperature gradient in space leading to large thermal stress and component fatigue. Precipitated by pipe break with jet impinging on structure or change in load with temperature transient at turbine inlet or mixing junction.
P8. Thermal Striping	High frequency temperature change can induce material fatigue.
P9. Abrupt Flow Change	Hydraulic loads may be imposed on structures. Turbine deblading may block turbine flow passages and precipitate large change in flow.
P10. Multi-Fluid Coolant	Air or water ingress after a leak may alter heat transfer and reactivity characteristics.

Table V List of Phenomena and Potential Design Issues (continued)

P11. Inter-Process Stability	Natural within-process time delays can lead to resonances between processes in the absence of active control elements. Stability needs to be investigated for nuclear-chemical plant coupling.
P12. Decay Power Level as a Function of Time	Under-prediction of core heat generation rate can result in elevated structure temperatures and material creep.

Table VI Major Phenomena as Identified by Operating Regime and Component in Primary Coolant Circuit

		Inlet Plenum	Core	Reactor Cavity Cooling Sys. Duct	Outlet Plenum	Hot Duct	Turbine	Turbine Inlet and Outlet Pipes	Recuperator	H$_2$ Process Heat Exchanger	H$_2$ Process Heat Exchanger Piping
Operating Regime	OR1										
	OR2		P9		P2a, P8	P6, P7		P6, P7	P7	P11	P7
	OR3	P1	P1, P2, P12	P3, P4, P5							
	OR4	P1	P3, P4	P3, P4, P5							
	OR5		P10, P12								
	OR6	P1	P1, P2, P10, P12	P3, P4, P5							
	OR7	P1	P10	P3, P4, P5							

Table VII Partial List of Design/Safety Issues in VHTR.

Operating Regime	Component	Phenomena	Design/Safety Issue
OR7 - *Depressurized / Conduction Cooling / Neutronic Power*	Inlet Plenum	P1 - *Thermal Stratification in Plenum.* Hot plumes rising from prismatic blocks will create stratified region at top of inlet plenum.	Poor mixing at top of inlet plenum may result in elevated temperatures and material creep.
OR4 - *Normal Pressure / Conduction Cooling / Neutronic Power*	Core - Coolant Channels	P3 - *Laminar-Turbulent Transition Flow* Transition region flow lies in the continuum between the laminar and turbulent flow regions.	Heat transfer and pressure drop in core channels may be underestimated resulting in higher fuel temperatures than otherwise.
OR4 - *Normal Pressure / Conduction Cooling / Neutronic Power*	Core - Coolant Channels	P4 - *Forced - Natural Convection Flow* Significant buoyancy-driven flow may develop taking friction pressure drop and heat transfer out of either the turbulent convection or laminar convection regime into the mixed convection regime.	Heat transfer and pressure drop in core channels may be underestimated resulting in higher fuel temperatures than otherwise.
OR4 - *Normal Pressure / Forced Convection Cooling / Neutronic Power*	Outlet Plenum	P8 - *Thermal Striping* P2 - *Jet Discharging Into a Plenum*	Hot and cold coolant channels - Variation in temperature between adjacent core coolant channel outlets can lead to thermal striping problems in the outlet plenum.

Inlet orificing and misplaced fuel blocks - The wrong flow can lead to overheating or overcooling which can lead to thermal striping problems in the outlet plenum. |

Table VII Partial List of Design/Safety Issues in VHTR (continued)

Operating Regime	Component	Phenomena	Design/Safety Issue
OR4 - *Normal Pressure / Forced Convection Cooling / Neutronic Power*	Core – Support Structures	P8 - *Thermal Striping*	Hot and cold coolant channels - Variation in temperature between adjacent core coolant channel outlets can lead to thermal striping problems. Inlet orificing and misplaced fuel blocks - The wrong flow can lead to overheating or overcooling which can lead to thermal striping problems.
OR4 - *Normal Pressure / Forced Convection Cooling / Neutronic Power*	Hot Duct	P6 - *Spatially Non-Uniform Heat Flow in Thick-Walled Structure at Steady State*	Permeation of hot gas into the duct insulation and into direct contact with the structure.
OR4 - *Normal Pressure / Forced Convection Cooling / Neutronic Power*	Turbine Inlet and Outlet Pipes	P7 - *Temperature Profile in Thick-Walled Structure During Transient*	When electrical load is dropped, turbine overspeed is avoided by flow bypass around the turbine. This creates temperature transients in the bypass line and turbine inlet and outlet pipes. Thermal stresses may be an issue depending on the wall thickness of these components.
OR4 - *Normal Pressure / Forced Convection Cooling / Neutronic Power*	H_2 Process Heat Exchanger		
OR4 - *Normal Pressure / Forced Convection Cooling / Neutronic Power*	H_2 Process Heat Exchanger Piping	P6 - *Spatially Non-Uniform Heat Flow in Thick-Walled Structure at Steady State* P7 - *Temperature Profile in Thick-Walled Structure During Transient*	

Table VII Partial List of Design/Safety Issues in VHTR (continued)

Operating Regime	Component	Phenomena	Design/Safety Issue
OR6 - Depressurized/ *Conduction Cooling/ Shutdown Decay Heat*	RCCS Duct	P4 - *Forced-Natural Mixed Convection Flow*	Under mixed convection conditions, heat transfer coefficient for heat flow from hot interior surface of duct into bulk air may be underestimated if natural or forced convection is assumed.

Table VIII   Structure of Phenomena Identification and Ranking Table

Transient Progression ↓	Phenomena in Each Operating Regime	Ranking of Phenomena				
		Component 1	Component 2	Component 3	Component 4	Component 5
Operating Regime 1	Phenomenon 1.1					
	Phenomenon 1.2					
	Phenomenon 1.m					
Operating Regime 2	Phenomenon 2.1					
	Phenomenon 2.2					
	Phenomenon 2.n					
Operating Regime 3	Phenomenon 3.1					
	Phenomenon 3.2					
	Phenomenon 3.p					

Table IX Heat Transfer and Pressure Drop Dependence on Dimensionless Numbers for Laminar Flow between Vertical Parallel Plates

	Pressure Drop	Heat Transfer
Forced Convection	$f = \dfrac{6}{Re}$	$Nu = \dfrac{h\,y_0}{k} = \dfrac{\partial\left(\dfrac{T-T_m}{T_0-T_m}\right)}{\partial\left(\dfrac{y}{y_0}\right)}$
Natural Convection	-	$v* = \dfrac{v_x \rho C_p y_0}{k}$ $Gr = \dfrac{g\,\beta\,y_0^{\;3}\,(T_1-T_m)}{v}$ $y* = \dfrac{y}{y_0}$ $Nu = \dfrac{h\,y_0}{k} = 1$

Table X Fuel Element Coolant Hydraulic Conditions as a Function of Operating Regime

Regime	Channel Normalized Flowrate	Channel Flowrate (kg/s)	Pressure (MPa)	Bulk Temperature (C)	Viscosity (µPa-s)	$Re = \dfrac{wD}{\mu A}$
Full Power	1.0	0.023	7.0	745	45	41,000
Pressurized with Shutdown Circulator	0.045*	0.0010	5.0	(807+341)/2= 574*	41	1,800
Depressurized with Shutdown Circulator	0.01*	0.00023	0.1	(1032+179)/2= 605*	42	410

* Based on Shutdown Cooling System performance given in [1].

Table XI Fuel Element Coolant Thermal Conditions as a Function of Operating Regime

Regime	Noramalized Power	Pressure (MPa)	Bulk Temperature (C/K)	Wall Heat Flux, q" (Mw/m²)	Density, ρ (kg/m³)	Coefficient of Volumetric Thermal Expansion, β (1/K)	Viscosity, μ (µPa-s)	Thermal Conductivity, k (W/m-K)	$Gr = \dfrac{g\rho^2 \beta q'' D^4}{k\mu^2}$
Full Power	1.0	7.0	745/1018	0.137 [a]	3.3	0.00098	45	0.37	1.2×10^6
Pressurized with Shutdown Circulator	0.059 [b]	5.0	574/847*	0.0081	2.8	0.0012	41	0.32	89,000
Depressurized with Shutdown Circulator	0.024 [b]	0.1	605/878*	0.0033	0.055	0.0011	42	0.33	12

* From Table VII. [a] From Table VI. [b] Based on Shutdown Cooling System performance given in [1].

Table XII Dimensionless Numbers for Fuel Element Coolant as a Function of Operating Condition

	Re	Gr	Gr Pr D/L[a]
Full Power	41,000	1.2×10^6	$\sim 10^4$
Pressurized with Shutdown Circulator	1,800	89,000	$\sim 10^3$
Depressurized with Shutdown Circulator	410	12	~ 0.1

[a] D/L is ratio of hydraulic diameter to channel length and is taken as 0.01

Table XIII   RCCS Duct Coolant Hydraulic Conditions at Reactor Full Power

Duct Air Flowrate (kg/s)	Pressure (MPa)	Average Bulk Temperature (C)	Viscosity (μPa-s)	$Re = \dfrac{wD}{\mu A}$
0.049	0.1	(43+274)/2 =159	23	14,000

Table XIV RCCS Duct Coolant Thermal Conditions at Reactor Full Power

Pressure (MPa)	Average Bulk Temperature (C/K)	Wall Heat Flux, q" (Mw/m^2)	Density, ρ (kg/m^3)	Coefficient of Volumetric Thermal Expansion, β (1/K)	Viscosity, μ (μPa-s)	Thermal Conductivity, k (W/m-K)	$Gr = \dfrac{g\rho^2 \beta q'' D^4}{k\mu^2}$
0.1	159/432	0.029	0.83	0.0023	23	0.035	1.15×10^9

Table XV Recommended values for empirical constants in the high Reynolds number k-ε model.

C_μ	C_1	C_2	σ_K	σ_ε
0.09	1.44	1.92	1.0	1.3

Table XVI RCCS Experiments [15]

Benchmark Problem	I	II	III	IV	VI-a	VI-b
Gas		Helium	Nitrogen	Helium	Helium	Helium
Pressure, MPa	1.3×10^{-6}	0.73	1.1	0.47	0.96	0.98
Heat Input, Total, kW	13.14	28.79	93.93	77.54	2.58	7.99
Segment 1, kW	1.01	1.16	5.90	5.63	0	0
Segment 2, kW	2.31	3.11	16.05	19.60	0	0
Segment 3, kW	2.64	3.52	19.88	21.59	0	0
Segment 4, kW	2.46	5.10	22.24	22.70	0	0
Segment 5, kW	3.76	10.42	22.13	0	0	0
Segment 6, kW	0.96	5.49	7.72	8.00	2.58	7.99
Cooling Panel	Water	Water	Water	Water	Air	Air
Stand Pipes	No	No	No	With	With	With

Table B.1 Summary of Outlet Plenum Experiments

Experiment	Organization	Feature	Reference Numbers
1	JAERI HTTR Experiments	Without mixing promoter	17, 18
2	JAERI HTTR Experiments	With mixing promoter	19
3	JAERI HTTR Experiments	With mixing promoter	20
4	JAERI VHTR Experiments	2 concentric nozzles	21
5	Chinese HTR-10 Experiments	A few mixing promoter options	22
6	German HTR-Module Experiments	2 core bottom & mixing promoters options	23

Table B.2 Conditions of Outlet Plenum Experiments

Experiment	Fluid	Geometry	Scale	Temp., C	Pressure, MPa	Flow Rate, kg/s	Reynolds Number	Measured items
1	helium	Core bottom structure	1:1	400-1050	1.0-4.0	1.0-4.0		Temperatures of helium gas in hot plenum
2	helium	Core bottom structure	1:1	300-400	~2-4		~$1.8\text{-}4.7 \times 10^5$	Temperatures of helium gas in hot plenum
3	water	Core bottom structure	1:7	25-65	0.1		$0.4\text{-}1.0 \times 10^5$	Water temperatures in hot plenum
4	air	2 concentric nozzles		~20-50	0.1			Air temperatures of the mixing stream
5	air	Hot gas chamber, core bottom structure, & hot gas duct	1:1.5	20-90	0.1	Typ. 1.68 Max. 2.44	$1.4\text{-}5.8 \times 10^5$	Air flow rates, temperatures, and differential pressures
6	air	Core bottom structure	1:2.9	$\Delta T \leq 40$	0.1		$0.59\text{-}1.8 \times 10^6$	Air temperature, pressure, and velocity